INVESTIGATION OF WIDE-BASE-SINGLE TIRE SAFETY AND STABILITY OF TRUCK

JITTRIN NIMITPERMPOON

A THESIS SUBMITTED IN PARTIAL FULFILLMENT
OF THE REQUIREMENT FOR THE DEGREE OF
MASTER OFENGINEERING IN AUTOMOTIVE ENGINEERING
(INTERNATIONAL PROGRAM)
INTERNATIONAL COLLEGE
KING MUNGKUT'S INSTITUTE OF TECHNOLOGY LADKRABANG
2017

KMITL-2016-IC-M-004-006

INVESTIGATION OF WIDE-BASE-SINGLE TIRE SAFETY AND STABILITY OF TRUCK

JITTRIN NIMITPERMPOON

A THESIS SUBMITTED IN PARTIAL FULFILLMENT
OF THE REQUIREMENT FOR THE DEGREE OF
MASTER OFENGINEERING IN AUTOMOTIVE ENGINEERING
(INTERNATIONAL PROGRAM)
INTERNATIONAL COLLEGE
KING MUNGKUT'S INSTITUTE OF TECHNOLOGY LADKRABANG
2017

KMITL-2016-IC-M-004-006

THESIS TITLE	Investigation of Wide-Base-Single Tire Safety and Stability of Truck
STUDENT NAME	Mr.Jittrin Nimitpermpoon
STUDENT ID	55600903
DEGREE	Master of Engineering
PROGRAME	Automotive Engineering
ADVISOR	Asst.Prof.Dr.Monsak Pimsarn
CO-ADVISOR	Prof.Hiroshi Yamaura
CO-ADVISOR	Dr.Sittikorn Lapapong

ABSTRACT

Because truck usage in Thailand tends to increase every year, fuel consumption needs to be a cause of concern to reduce pollution as well as the cost of fuel. According to most research, a Wide-Based-Single tire (WBS tire) can significantly reduce fuel consumption. However, the vehicle dynamics analysis shows that the tire is one of the most important components that have a strong effect on vehicle control. Therefore, changing the tires may affect the stability of a truck. The semi-empirical model, "Magic Formula" was one of the most famous tire models used in vehicle dynamics. However, it requires a testing procedure that is both costly and time consuming. The classical analytic tire model, "Brush Model," also has a lot of error, especially for high slip angle. This article utilizes the "Cold-Hot Friction Law" to improve the calculation of the Classical Brush Model. The calculated results show that the proposed tire model can reduce errors from 11% to 6.23% at 4 degrees of slip angle and from 8% to 0.6% at full-slip when compared to FEA results. Calculation time was also reduced significantly, from 1 hour to less than 5 minutes. After applying the calculation to a WBS tire, the results showed that the WBS tire generated less cornering stiffness when compared to dual tires. Therefore, a truck that uses WBS tires needs to adjust the weight distribution more to the front of the vehicle, in this case 3%, to maintain cornering performance.

KEY WORDS: Tire, Wide-Based-Single Tire, Friction Model, Tire Force Estimation, Cold-Hot Friction Law

ACKNOWLEDGEMENTS

This thesis could not have been accomplished without the assistance of certain people. Thank you so much to the advisors, Asst. Prof. Dr. Monsak Pimsarn, Prof. Hiroshi Yamaura, and last but not least, Dr. Sittikorn Lapapong, who provided great help during every process of completing this thesis. I really appreciated the time and effort each advisor put into helping me to work through it and finish it.

My gratitude goes to the TAIST-Tokyo Tech program and National Science and Technology Development Agency (NSTDA), who provided a scholarship for registration fees and the course work as well as conference.

The research budget and support mainly came from Research and Researchers for Industries (RRI) and Michelin Siam Co., Ltd. Thank you so much for your kind cooperation, even if this thesis took a very long time to be done.

Testing data for the FSAE tires came from the Milliken Research Centre and was provided by the Automotive Club of King Mongkut's Institute of Technology Ladkrabang, also known as the "Initial Team." Thank you to those hard working students and the club's advisors, Asst. Prof. Dr. Chinda Charoenpornpanich and Dr. Preechar Karin, who also provided invaluable support for this thesis.

To Mr. Niwat Phoocharoen, who always gives help whenever I have a problem. I really appreciate your help in many ways, not only in the thesis procedure. Thank you very much.

To my dear friends and family, thank you for your support in pushing me to move on until I could finish this work. I was finally able to finish this thesis and am ready for graduation. Without your help, I could never have done it. Thank you so much.

TABLE OF CONTENTS

TABLE OF CONTENTS

(Continued)

Chapter **Page**

TABLE OF CONTENTS

(Continued)

Chapter **Page**

LIST OF TABLES

Table **Page**

TABLE OF FIGURES

Figure **Page**

TABLE OF FIGURES

(Continued)

Figure **Page**

TABLE OF FIGURES

(Continued)

Figure **Page**

LIST OF SYMBOLS

l	Footprint length
b	Footprint width
x	Longitudinal distance from leading edge
y	Lateral distance from wheel center
F_x	Longitudinal tire traction force
F_y	Lateral tire traction force
F_z	Vertical load of the tire
M_z	Self-aligning torque generated from tire
s	Input of "Magic Formula" after graph shifting
S	Actual input of "Magic Formula"
S_V	Vertical graph shifting value
S_H	Horizontal graph shifting value
o	Output of "Magic Formula" after graph shifting
O	Actual output of "Magic Formula"
B, C, D, and E	Constant of "Magic Formula"
κ	Longitudinal slip (Slip Ratio)
α	Slip angle of the tire
γ	Camber angle
ν	Lateral tire deformation distance
V	Vehicle speed

μ	Static friction coefficient
μ_D	Dynamics friction coefficient
μ_{Hot}, μ_{Cold}	Friction coefficient for "Cold-Hot Friction Law"
μ_{Eff}	Effective friction coefficient
P	Pressure
P_m	Maximum pressure in footprint area
c_{py}	Tire lateral stiffness
C_{10}, C_{20}, C_{30}	Yeoh's Model constants

CHAPTER 1

INTRODUCTION

1.1 Wide-Base-Single Tire

According to the Department of Land Transport (DLT) of Thailand (1)[1], the number of trucks registered with the Thai government is currently over 1 million, having increased each year since 2005. A statistical graph of total trucks registered is shown in Figure 1.1. Truck usage has increased in correlation with the increase of industrial activities and changing government policy.

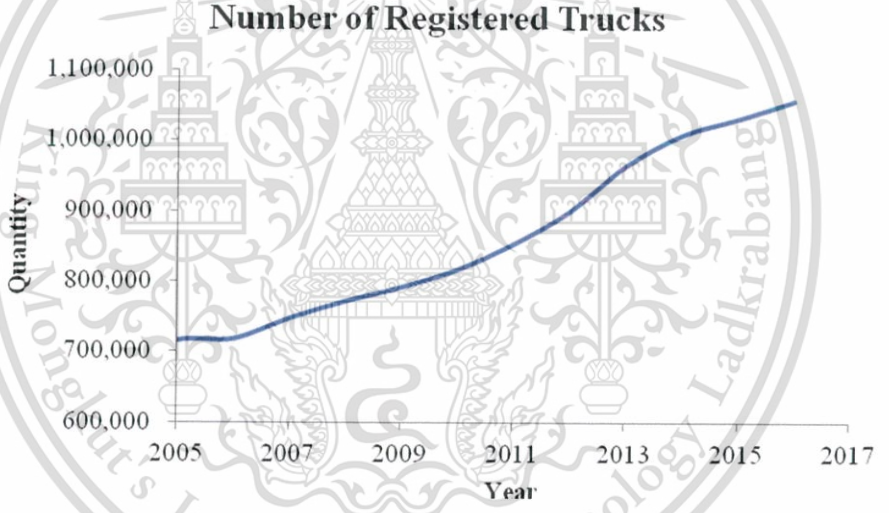

Figure 1.1 Statistics for total number of registered trucks in Thailand between 2005 and 2017 **[1]**

According to data from truck service centers, trucks are on duty for over 100,000 km each year. Average fuel consumption for a truck is 3 km/liter, which equates to roughly 33.3 billion liters of total fuel consumption each year. What is more, this number is likely to increase every year. For truck usage, resistance occurs from many sources, i.e. Aerodynamic Resistance, Mechanical Loss, Rolling Resistance, etc. According to many researches, a Wide-Based-Single (WBS) tire can reduce overall fuel

consumption around by 1% to 8% [1] [2] [3] [4]. By supposing on the share market, it can be assumed that 10% of total trucks have changed to the use of WBS tires. Therefore, approximately 100,000 trucks have reduced their fuel consumption by around 4%, which is equal to 133.2 million litres of fuel usage reduced each year and equal to 2.664 billion THB (estimated at 20 THB per litre). This rough assumption shows that WBS tires offer significant improvement on fuel consumption and fuel import costs in Thailand.

Figure 1.2 Effect of WBS tires on fuel and energy economy in Thailand

1.2 Role of Tires in Vehicle Dynamics

Land vehicle usage also comes with pneumatic tire usage. Since driving force, braking force, and cornering force are generated by the tires, tire force plays a major role in the analysis of vehicle dynamics. Driver assistance systems, i.e. Anti-Lock Brake Systems (ABS) [6], Rollover Prediction [7], and Electronic Stability Programs (ESP) are also related to tire slip phenomenon. Therefore, an analysis of a Human-Vehicle-Road system must have the tire as one of the most important components that affect the system because the tire is the component that contacts the road surface and generates every force used to control the vehicle.

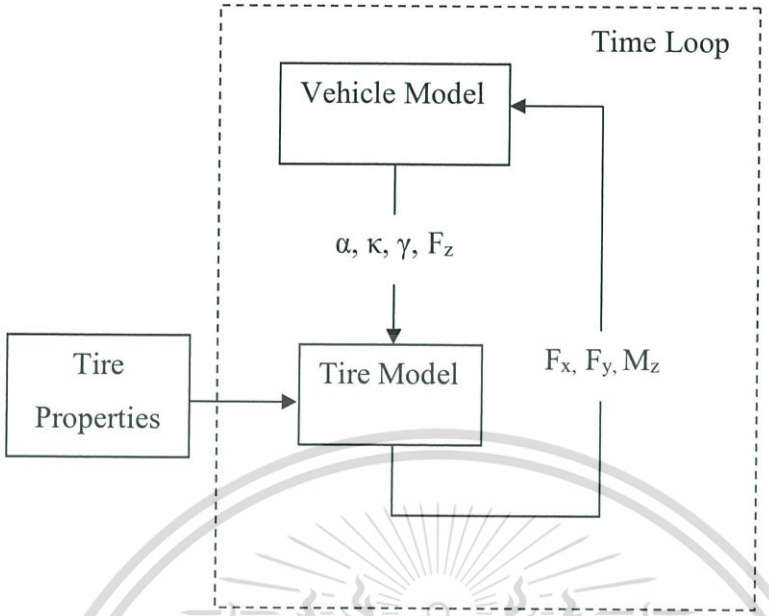

Figure 1.3 Simple Vehicle Dynamics calculation diagram

As shown in Figure 1.3, the role of the tires in Vehicle Dynamics is one of the major calculations since they give feedback about overall vehicle performance and work as the external force generators. Therefore, almost every external force will depend on tire properties. Each tire has its own characteristics and properties. When a tire is changed, the vehicle properties also change, which will also affect the Vehicle Dynamics analysis [4].

As mentioned in Section 1.1, WBS tires can improve fuel economy. However, tires are also involved with vehicle dynamics and the driver assistance system. Tire changes can offer a significant effect on vehicle stability, driving experience, and safety. When changing tires, tire force and tire properties must also be concerned.

1.3 Tire Force Characteristic

Throughout this article, the tire coordinate system will be referred to as SAE standard. The diagram below shows the tire on the ground that has a camber angle and slip angle. Longitudinal Force, Lateral Force, and Vertical Load are represented as F_x,

F_y, and F_z, respectively. The Overturning Moment, Rolling Resistance Moment, and Self-Aligning Moment are represented as M_x, M_y, and M_z, respectively.

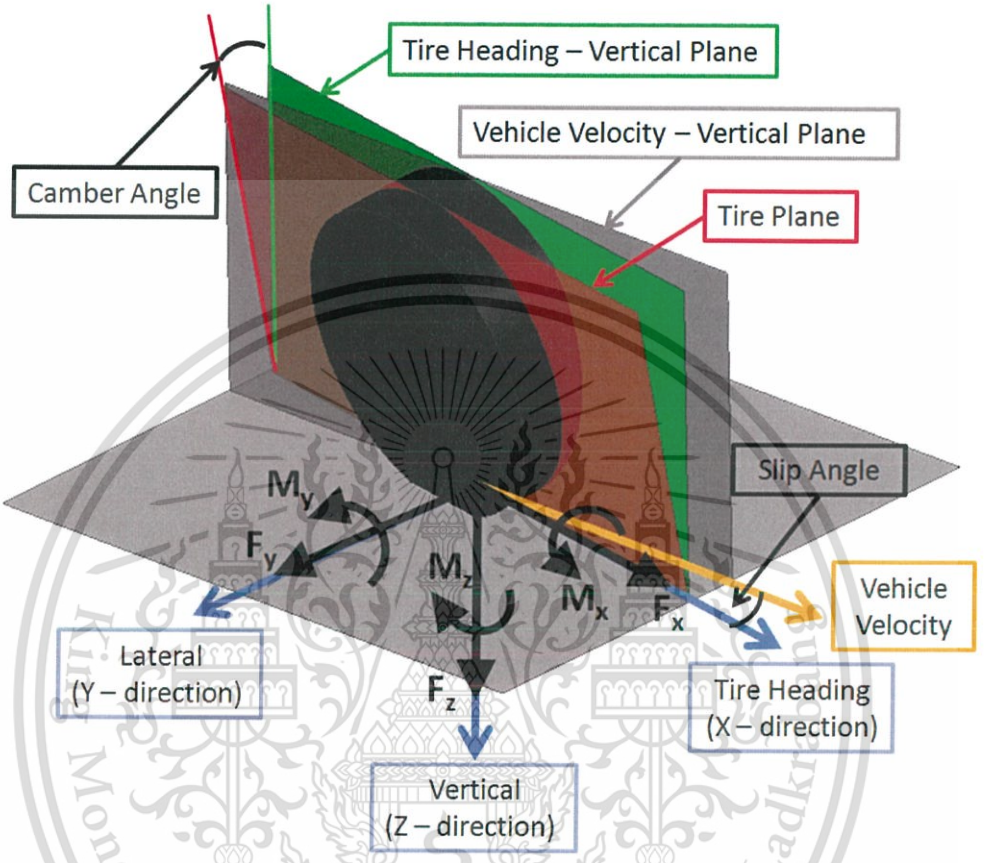

Figure 1.4 Tire coordinate system, force, and torque definition refers to SAE **[9]**

Tire model primarily comes with inputs and outputs, as shown in the figure below. The inputs used in the tire model are Vertical Load (F_z), Camber Angle (γ), Longitudinal Slip (κ), and Slip Angle (α). The results from tire model will give Longitudinal Force (F_x) and Lateral Force (F_y) as the forces that control the vehicle. Self-Aligning Torque (M_z) gives the reaction torque in the steering wheel. Therefore, the feeling of steering wheel control refers to this parameter.

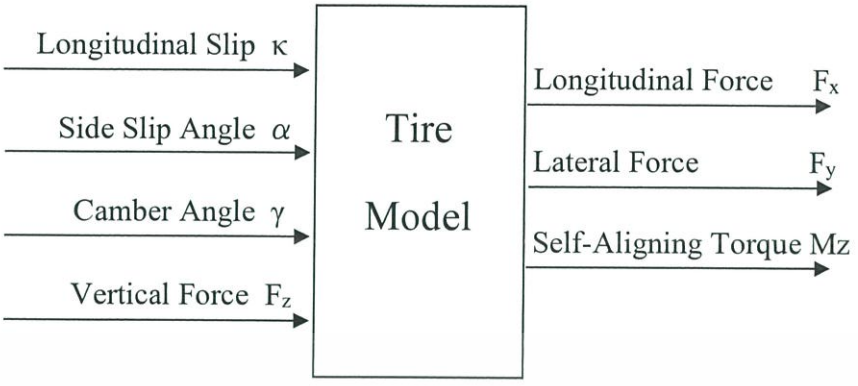

Figure 1.5 Tire Model input and output

The Slip Ratio or Longitudinal Slip is defined from the ratio of the wheel rolling speed compared to actual vehicle speed, as see in Equation 1.1, which occurs primarily during acceleration or braking of the vehicle.

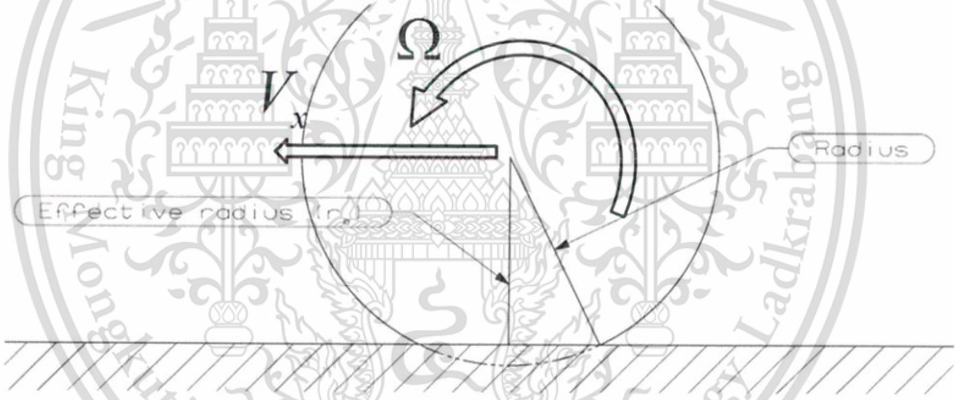

Figure 1.6 Longitudinal Slip (Slip Ratio, κ) definition

$$\kappa = \frac{r_e \Omega - V_x}{V_x} \tag{1.1}$$

One of the methods used to explain tire slip-force is testing on a tire testing machine such as Calspan [10]. The testing results can be derived into a mathematical model called "Magic Formula" or "MF-Tire Model" [10] [11] [12]. This method is very accurate and used widely in simulation programs, i.e. MSC. ADAMS, Car Sim, etc. However, the testing method used to achieve the input data is costly and time

consuming. Furthermore this method is more like curve fitting [2], which does not represent the physical meaning of rubber contact mechanisms or other phenomenon that actually happens during slip occurrence.

Another slip-force graph can be achieved by analytical method considering the mechanical properties of the tire. The tire model called "Brush Model" [13] [10] is one of the most popular calculations widely used. The calculation is done on simple assumption. From the calculation results, this method is not enough to explain every phenomenon, such as the effect of tire width on maximum lateral force or traction loss at full-slip. Further information will be discussed in Chapter 3.

Another option used nowadays is Finite Element Analysis (FEA) [9] [10] [14]. By using many complex mathematical models together, this method can provide high accuracy in tire force prediction. To achieve accurate results, however, good understanding of both the theorem behind the calculation and the tools used in the program need to be gained first. Because the calculation of the tire slip-force involves a dynamics simulation, it will result in the requirement of a high performance computer and high calculation time. Furthermore, the simulation results will not be accurate if the mathematical models chosen for use of the calculations are not appropriate.

1.4 Thesis Outline

Chapter 3.1 will show the calculation results and major problems of the Classical Brush Model. The chapter will move on to improvement of the model in Chapter 4.1 through 4.6. The improvement will consist of 3 parts: Footprint and Pressure Distribution, Tire Lateral Stiffness, and Friction Model. Essentially, each parameter gives an effect on the calculation result. Finally, the completed proposed tire model will be detailed in Chapter 4.7.

Validation will be shown in Chapters 5.1 and 5.2. The calculation results for truck tires will be shown in Chapter 5.3, while the vehicle dynamics evaluation will be shown in Chapter 5.4. The discussion and conclusion will be presented in Chapter 6.

CHAPTER 2

LITERATURE REVIEW

In Chapter 2.1 to 2.3 will be some details given of tire modeling widely used nowadays. Each of the methods has its own strengths and weaknesses. To choose the method appropriately, basic understanding of each method is required.

Chapter 2.4 will introduce rubber friction modeling, which has a major role in this article. The research in rubber friction could give physical explanations and improve calculation results significantly.

2.1 Semi-Empirical Model

The Magic Formula was first introduced in 1987 by Bakker et al. [11]. The calculation related to steady-state tire tests resulting in pure-slip case. The calculation needs a set of testing data for 3 different vertical loads in at least 3 relationships of parameters. That means at least 9 tests needs to be done, which could potentially consume time and costs for both prototype preparation and testing procedure. The testing results will be used to carry out curve fitting and find the constants for the Magic Formula. The Magic Formula could give accurate tire force prediction because it's done based on the testing result. However, it is only appropriate for steady-state pure-slip cases.

In 1993, Pacejka et al. [10] introduced a newer version called the Magic Formula Tire Model (MF-Tire Model), which included the combined slip into the calculation. This offers improvement for the calculation in non-steady-state cases. The testing procedure is quite complicated and consists of at least 20 tests. The evaluation for the coefficient in the Magic Formula Tire Model consists of around 80 equations to calculate for the complete Magic Formula Tire Model. This tire model may give more flexibility in vehicle dynamics analysis, but the tire data is costly and time consuming.

2.2 Analytical Model

The Brush Model was first published in 1952 by Hadekel [10]. The model explained that tire traction occurred from the deformation of the tread element. Lateral force and self-aligning torque are generated by tread deformation acted by the slip angle. The calculation is based on a simple assumption and the calculation result shows that it cannot predict the traction loss at full-slip. Further, the self-aligning torque will not be less than 0. Since the calculation is very simple, calculation time is very low and each calculation procedure also represents the physical meaning. If the model has been evaluated properly, it can be improved by the physical model proposed in previous research. The details of the Classical Brush Model are shown in Chapter 3.

2.3 Finite Element Method

In 2000, K. Kabe and M. Koishi [23] introduced the Finite Element Method using a commercial code named ABAQUS. The calculation included Hyperelastic, Viscoelastic, and Composite Structure. The calculations were done to evaluate slip-angle vs. lateral force and slip-angle vs. self-aligning torque for the slip angle at 0, 1, 2, and 3 degrees. The results could predict lateral force and self-aligning torque precisely with an error of only 8% compared to experiments. However, the calculation time for explicit dynamics and implicit dynamics is 192 hours and 6.5 hours, respectively.

In 2001, E. Tönük and Y. S. Ünlüsoy[14]conducted research about lateral force vs. slip-angle of radial passenger tires using commercial FEA code, MSC. Marc. The research included only Hyperelastic material and rebar-type composite structures. The Viscoelastic material property was excluded to keep the calculation simple. The Coulomb Friction model was used in the calculation. The slip angle varied from 0, 1, 2, 3,…, 8 degrees. The vertical load varied from 1500, 2000, 2500, …, 4500 Newton. The calculation time was not presented in the research. The calculation results provided a low level of error at around 5%.

In 2011, X. Yang[9]carried out research using commercial FEA code, ABAQUS, to predict the cornering force of the Formula Student Tire. In the research,

Yang tested a tire to get the material properties for each section of the tire structure. The calculation was done using the Yeoh Model for Hyperelastic material, Mooney-Revlin Model for Viscoelastic material, and rebar composite type for steel reinforcement. The contact mechanics of tire and road used Coulomb Friction. The calculation varied the slip angle from 0, 1, 2, 3,...to 6 degrees. The calculation results could give low error of around 7%. The calculation time for lateral force was not shown, but for footprint analysis only, around 30 minutes was required for completion.

2.4 Tire Friction Model

From 1998 through 2013, BNJ Persson conducted research on the contact mechanism of rubber material and tire-road contact [2][15] [18] [19]. The research mainly explained rubber friction as affected by temperature. Since rubber tires are made of Viscoelastic material, the deformation of the tread will generate heat on its contact surface.

In 2006, the "Flash Temperature Model" was proposed [19]. The model consisted of many complex equations and was hard to evaluate. The main idea was to explain about the energy dissipation that occurred during slipping of a rubber block on a rough surface. The surface roughness was evaluated by a power spectrum function with wave length as input. Since the asphalt surface is self-affiliated, the cut-off wave length q can be evaluated by plotting C-q graph. Majorly, the road will have a similar cut-off wave length because they are all made from similar sized stones. The effect of "Flash Temperature" will give a more pronounced effect at higher speed. This is because the energy can be diffused to ambient air at lower speed.

In 2010[2], "Cold-Hot Friction Law" was proposed as a simplified version of "Flash Temperature Model." The calculation results based on "Cold-Hot Friction Law" gave similar results with the calculation done by "Flash Temperature Model."However, "Cold-Hot Friction Law" is far less complex. The calculation was done by using the pressure distribution profile from static load testing. Tire modeling was done on 2-dimensional dynamic analysis. The tread element has properties of constant axial

stiffness, constant bending stiffness, constant axial damping, and constant bending axial damping. The results could predict lateral force precisely and represent friction loss at full-slip. However, self-aligning torque prediction still has a high level of error. Persson gave suggestions that self-aligning torque error occurred from pressure distribution during tire slip, which may be different from the static pressure distribution used in the research.

2.5 Conclusions

After reviewing many researches, the evaluation of vehicle stability affected by tire changes can refer to a bicycle model. Using steady-state cornering and pure side-slip is enough to evaluate skid-pad cornering. This method can be used as a benchmark for tire performance evaluation.

The tire model used in this article will focus on the Brush Model, which requires low specification CPU and uses low calculation time. Further, this method can evaluate the tire-slip force as a nonlinear relationship.

A tire-road friction mechanism refers to "Cold-Hot Friction Law" because it has a simple mathematical model and is enough to evaluate rubber friction during non-stationary slip. Furthermore, the result in Persson's research, this model can represent the maximum lateral force that is affected by the footprint shape.

2.6 Objectives and Scope of Work

After conducting research, the author sees that the classical methods that have been used to predict tire traction are either costly or inaccurate. Tire-slip force modeling is mainly affected by contact mechanics. The contact mechanics modeling for rubber-like material is one of the topics of interest [15][2][16][17]. Even in FEA simulation, the simulation result can give high error if the contact model is not appropriate.

To achieve the most effective method, this article will focus on analytical method improvement because it is less costly and able to give physical meaning to the

tire-road contact mechanism. Furthermore, if the mathematical modeling is improved for analytical modeling, the modeling is also able to be included into FEA program to improve the calculation for tire-road analysis. After achieving the appropriate calculation modeling, it will be applied into the truck tire calculation to compare the tire properties between a normal dual tire and WBS tire.

2.6.1. Objectives

1) Investigate Classical Brush Model problems and propose a solution to improve the calculation
2) Find appropriate methods to predict tire force in the designing process without using the prototype
3) Compare tire performance between Wide-Based-Single Tire and Dual Tire in pure lateral slip case

2.6.2. Scope of Works

1) Evaluate tire slip-force graph in steady-state and pure side-slip case using an analytical method
2) Analyse the Classical Brush Model and improve the calculation
3) Validate the Proposed Tire Model with other research
4) Predict the slip-force graph of the WBS tire and normal dual tires
5) Use the slip-force graph to compare the performance of vehicle in skid-pad course with different tires

CHAPTER 3

CLASSICAL BRUSH MODEL PROBLEMS

Considering Figure 3.1, the testing result shows that the lateral force has slightly decreased at full-slip. This phenomenon will have greater effect on wider tires or with higher vertical load. The testing result also represents that a wider tire will generate higher lateral force and has higher cornering stiffness. The next step is to move on to the tire slip-force graph prediction by using an analytical calculation called the "Brush Model".

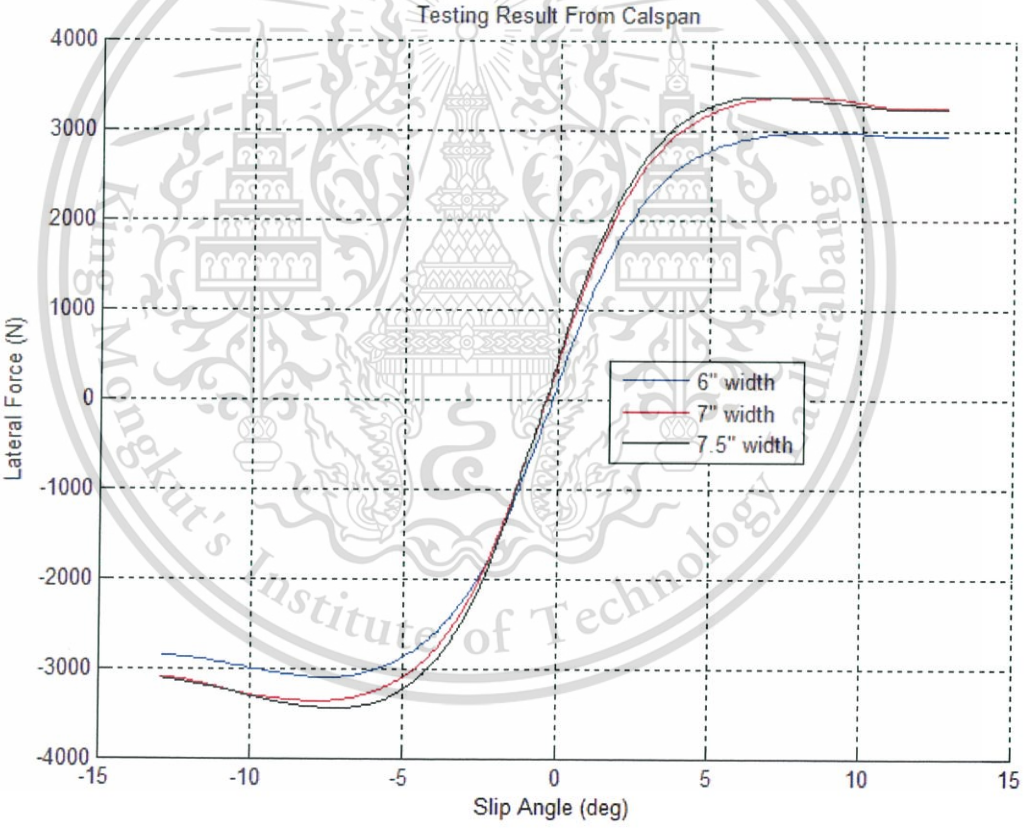

Figure 3.1 Lateral force testing result of different width tire

The Classical Brush Model calculation procedure has shown in figure 3.2. The main equation used in lateral force calculation is equation 3.1.

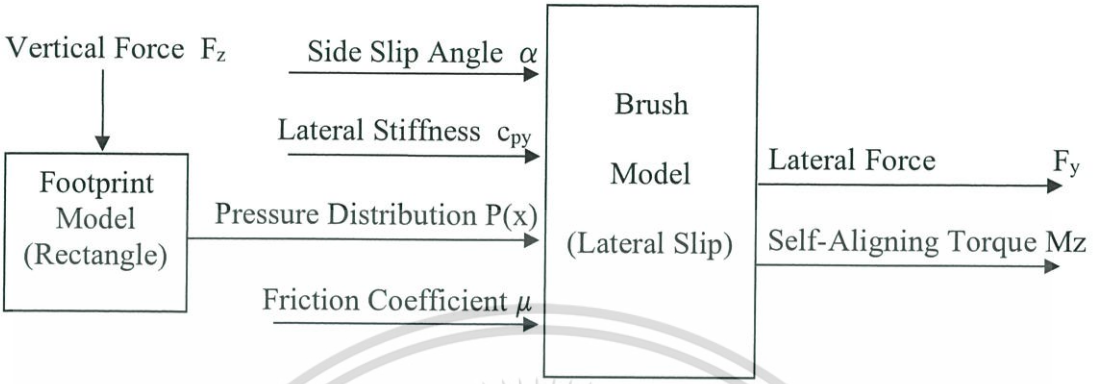

Figure 3.2 Classical Brush Model diagram

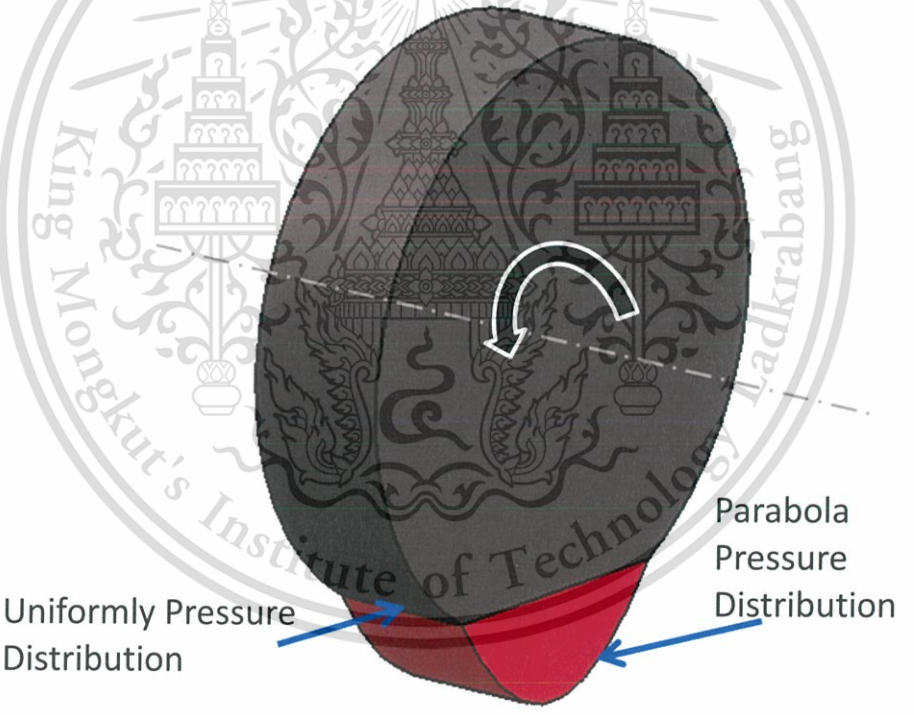

Figure 3.3 Pressure Distribution of Tire-Road Contact

$$F_y = c_{py} b \int_0^l v(x)dx \tag{3.1}$$

Since tread deformation (υ) can be calculated from slip angle of the thread. From leading edge, υ will increase from 0 until reaching the maximum tread deformation capability. Then, the tread will lose its traction and be restored back to its original position. Tread maximum deformation calculated from pressure acts on the tread element.

By assuming that pressure is distributed in the shape of parabola along the longitudinal axis, the pressure distribution can be calculated by Equation (3.2). By assuming that pressure is uniform along the lateral axis and the force is balance in the vertical axis, rearrange Equation (3.2) and (3.3), the P_{max} can be calculated from Equation (3.4):

$$P(x) = 4P_{\max}\left(x/l\right)\cdot\left(1 - x/l\right) \quad (3.2)$$

$$F_z = b\int_0^l P(x)dx \quad (3.3)$$

$$P_m = \frac{3F_z}{2bl} \quad (3.4)$$

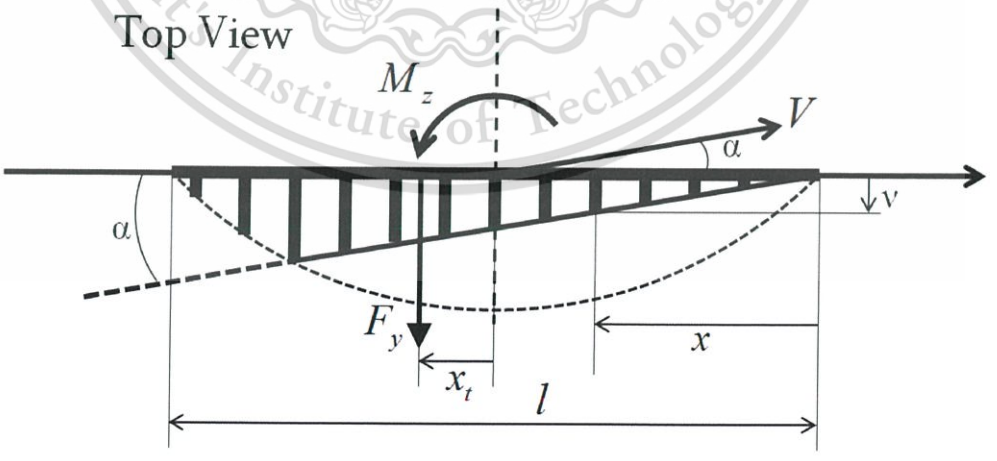

Figure 3.4 Top view diagram

$$v = \begin{cases} x\tan\alpha & \cdots AdhesionZone \\ \dfrac{\mu}{c_{py}}\left[\dfrac{4P_m}{l^2}\left(\dfrac{l}{2}-x\right)^2 + P_m\right] & \cdots SlipZone \end{cases} \quad (3.5)$$

$$M_z = c_{py} b \int_0^l v x_t dx \quad (3.6)$$

From Figure 3.4 and Equation (3.5), the Lateral Slip – Force can be evaluated. For self-aligning torque, the calculation will be take place by substituting Equation (3.1) with Equation (3.6). The calculation result for lateral force and self-aligning torque is shown in Figure 3.5

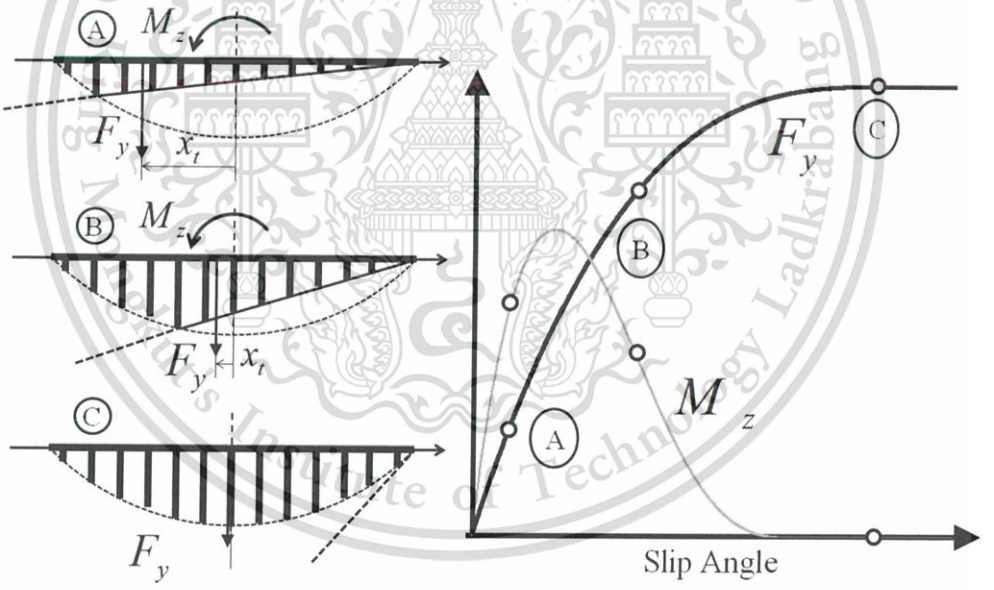

Figure 3.5 Lateral force and Self-Aligning torque from low slip to full slip

Considering Equations (3.2), (3.3), and (3.4), the P_{max} has been calculated from the force balance in the vertical axis. Therefore, total pressure in the footprint area will

be equal to F_z. Since Equation (3.5) at full slip will be $v(x) = \frac{\mu}{c_{py}}\left[\frac{4P_m}{l^2}\left(\frac{l}{2}-x\right)^2 + P_m\right]$ when substituted into Equation (3.1), the integral result will be $F_y = \mu \cdot F_z$

On the other hand, Equation (3.5) has P_m in common. Therefore, it can factor P_m out of the bracket. Since P_m is constant, Equation (3.1) is also able to place P_m outside the integration. P_m has b as a divisor, so it can cancel with b in Equation (3.1).

After considering both the mathematical and physical meaning of Classic Brush Model, this model cannot represent the width of a tire that affects Lateral Force at full-slip. To prove this hypothesis, the Classical Brush Model calculation will be done in MATLAB code and compared to the result with the calculations in a lecture document to check that coding is correct. Afterwards, the input data for tire footprint will change to see whether or not footprint width has any effect on the calculation result.

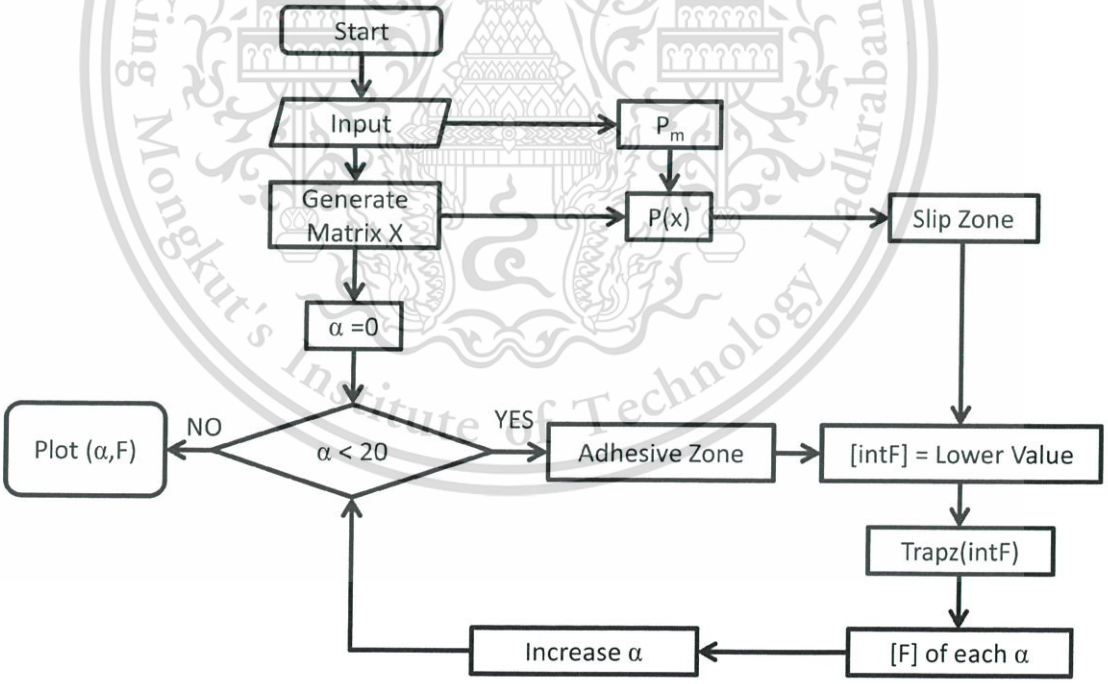

Figure 3.6 Flowchart of Lateral Force calculation

The calculation procedure is shown as a flowchart in Figure 3.2. Since the equation (3.1) has an integration form, the numerical method was chosen to solve the integration and to make the calculation simple and easy to change the inputs. Thex-direction will be generated as a matrix of positions from 0 to the length of the footprint (l). The slip angle (α) has to vary from 0 to design value; in this case, 20 degrees will be used. Substitute the matrix [X] and each value of α into Equation (3.5) for Adhesive Zone to get the deformation of tread element affected by each slip angle. After that, use vertical load (F_z), footprint length (l), and footprint width (b) with Equation (3.4) to calculate for maximum pressure (P_m). The Lateral Stiffness (c_{py}) and friction coefficient (μ) are input data also. Therefore, the equation (3.5) for Slip Zone can be calculated. The actual deformation of the tread element (v) will be the lower value in each x-position of the result from Equation (3.5). If-else logic will be used to choose the lower value and assign into matrix [intF], as well as use Trapezoid Rule to get the integration result for Equation (3.1).The input data is shown in Table 3.1.

Contact Shape	Contact Length, l (m)	Contact Width, b (m)	c_{py} (N/m)	Vertical Load, F_z (N)	μ
Rectangle	0.129	0.101	53.6×10^6	3,920	1

Table 3.1 Parameters for calculation in lecture, same length

The calculation result gives similar result, as shown in the lecture document. Since the calculation is done with a numerical method, the grid size may affect the result. The calculation is done again with a different size and checked for the result. The result of each grid size is shown in Table 3.2. Calculation Time is evaluated by using the "cputime" command in MATLAB.

The calculation result shows that the grid size of 0.1 mm is enough to approach accurate result and allow maintenance of low calculation time.

Size (mm)	Calculation Time (sec.)	Force at 3 degree (N)	Force at 5 degree (N)	Force at 10 degree (N)	Maximum Force (N)
10	0.4368	1,848.6	2,695.5	3,713.4	3,843.5
1	0.5460	1,918.4	2,767.6	3,785.7	3,919.8
0.1	0.7488	1,918.5	2,767.7	3,785.9	3,920
0.01	5.6160	1,918.5	2,767.8	3,785.9	3,920
0.001	39.951	1,918.5	2,767.8	3,785.9	3,920

Table 3.2 Calculation result and time of each grid size

After applying the classical brush model to calculate tires that have different width, the results are shown in Figure 3.7. The maximum lateral force that tires could generate is the same as expected. Only cornering stiffness increases relative to tire width. Compared to the testing result, the Classic Brush Model is still able to represent the effect of the tire width to cornering stiffness.

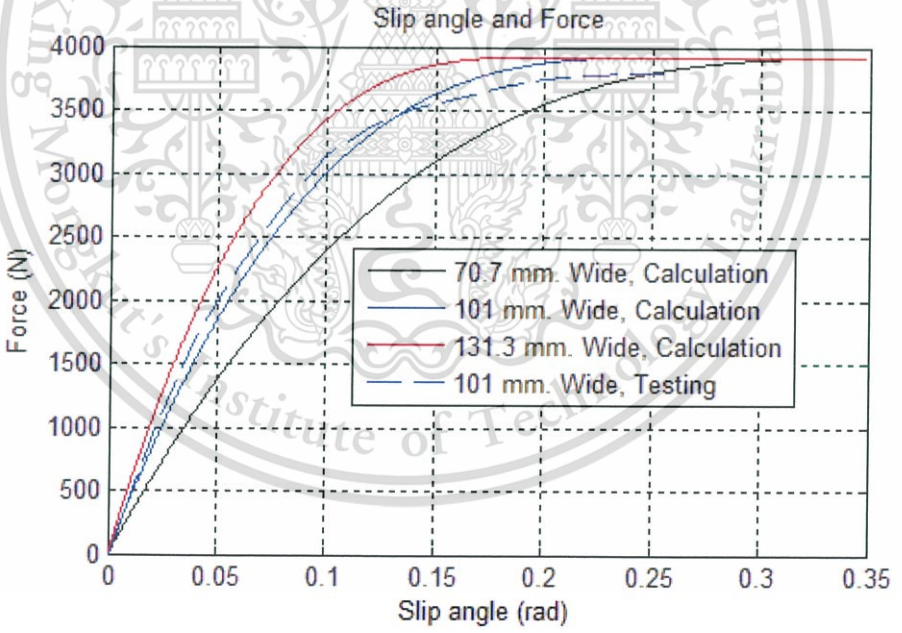

Figure 3.7 Lateral force calculated at different tire widths

Considering Equation (3.2) and (3.4), when the footprints have same length but different width, the maximum pressure, P_m, will be different. P_m will be decreased if the

footprint is wider. Further, the parabola shape will have the same base length since the footprint lengths are the same. The calculation result for pressure distribution is shown in Figure 3.3.

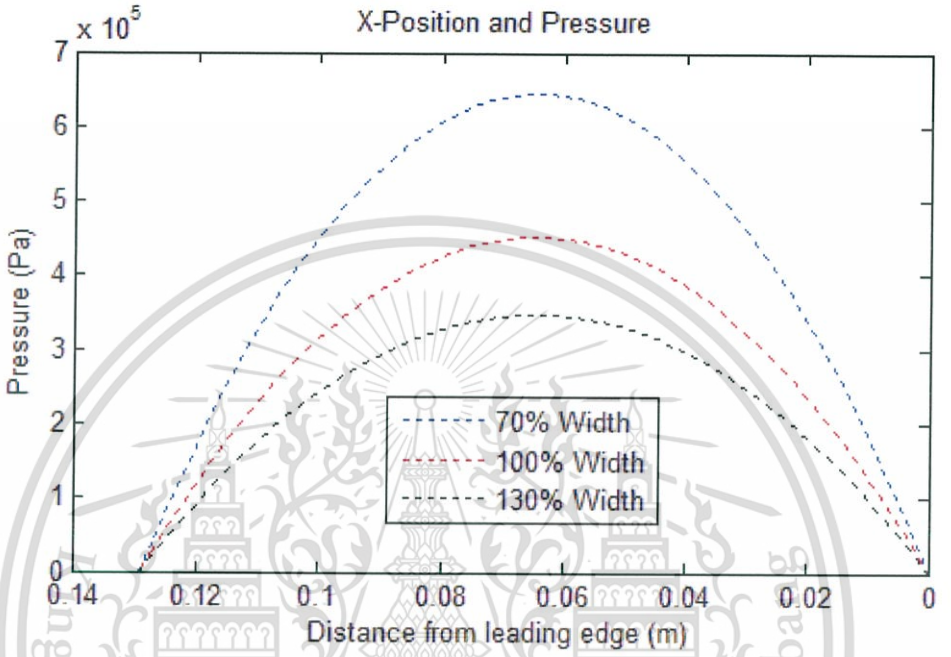

Figure 3.8 Pressure distribution in different footprint widths

As seen in Figure 3.3, a wider tire gives lower maximum pressure, as expected. From the equation (3.5), Lateral Force before full slip will consist of Adhesive Zone and Slip Zone. In Adhesive Zone, the equation will not involve P_m, meaning that when substituted into Equation (3.1), the wire width will not be cancelled out. That will result in the Lateral Force of the wider tire being higher than before full-slip. However, it will be full-slip at lower Slip Angle because the maximum pressure is lower and will affect lowering of the maximum thread deformation capability.

Another parameter that gives Pure Lateral Slip testing is Self-Aligning torque. From the testing result, a wider tire tends to generate higher torque. At full-slip, a tire can generate negative torque. The driver can experience this phenomenon as the steering wheel loses its counter-torque and the driver tries to pull the steering wheel further, resulting in loss of tire traction.

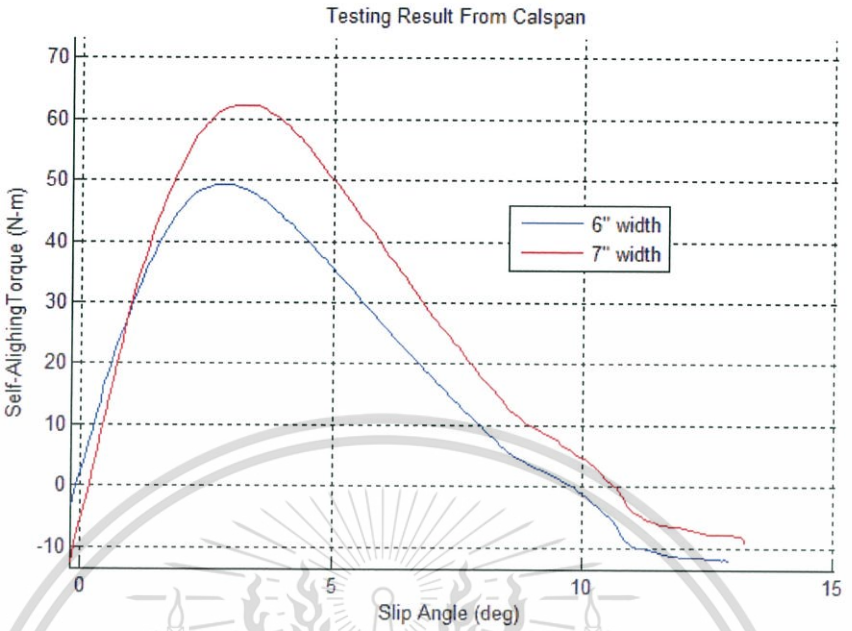

Figure 3.9 Testing Result of Self-Aligning torque

Considering Figure 3.4, the total force will always act on the left hand side of the wheel-rotating axis. That means the calculation result of M_z will always be a positive value. The result in the lecture document and in the book also supports this assumption.

The calculation of M_z is similar to F_y but before the integration process, each tread element will be multiplied by the distance from tire rotational axis first. The calculation flowchart is shown in Figure 3.10.

After carrying out the calculation, the value is always positive, as expected. The calculation result for the tire that has 101 mm width is the same as the result in the lecture document. The calculation programs can calculate properly. However, the result shows that a wider tire has less torque than a narrow tire. The effect of tire width from the calculation is contrary to the testing result. Furthermore, the maximum torque is also only half of the testing result.

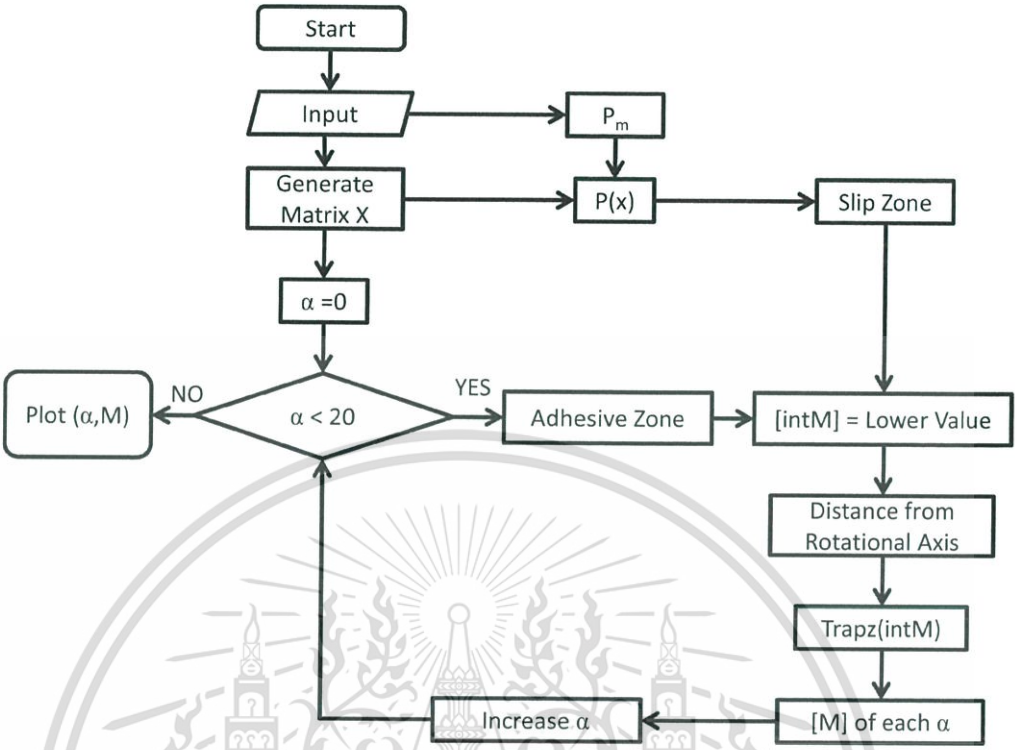

Figure 3.10 Flowchart of Self-Aligning Torque calculation

Size (mm)	Calculation Time (sec.)	Torque at 3 degree (N-m)	Torque at 5 degree (N-m)	Torque at 10 degree (N-m)	Maximum Torque (N-m)
10	0.5616	25.5686	24.7161	5.9694	26.5773
1	0.5616	25.9099	24.8999	5.8388	26.6616
0.1	0.7956	25.9144	24.9049	5.8415	26.6651
0.01	6.0684	25.9144	24.9050	5.8415	26.6652
0.001	43.8519	25.9144	24.9050	5.8415	26.6652

Table 3.3 Calculation result and time of each grid size

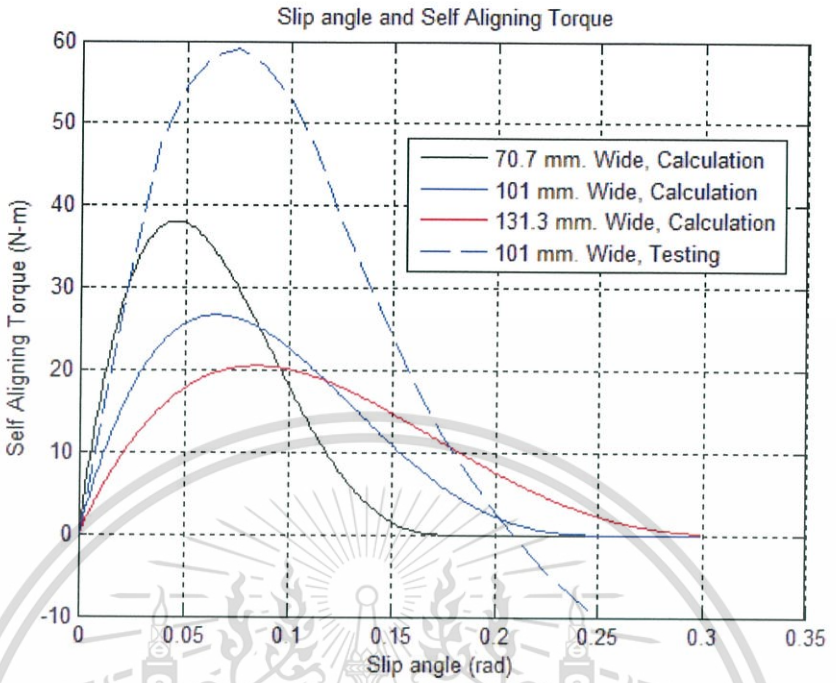

Figure 3.11 Self-Aligning torque calculated at different width

As the result shows, the Classic Brush Model couldn't properly calculate the Lateral Force of the tires that had different widths. Self-aligning torque also gavean unexpected result. To make the calculation more accurate, the Classic Brush Model needs to be improved.

Since the Classic Brush Model has been based on many simple assumptions, i.e. constant lateral stiffness, rectangles shape of footprint, etc. Chapter 4 will evaluate each parameter and substitute with better modeling to improve the model. Improvement will focus on Lateral Force first since it plays a major role in the vehicle dynamics evaluation, as mentioned in Chapter 1.

CHAPTER 4

PROPOSED TIRE MODEL

4.1 Introduction to Proposed Tire Model

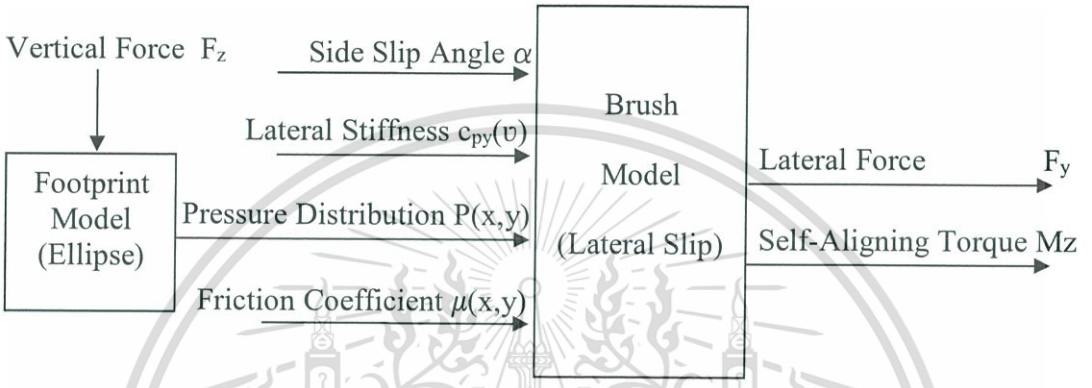

Figure 4.1 Proposed Tire Model diagram

After researching pneumatic tire phenomenon, classical tire brush modeling has been done on many rough assumptions. 1) The lateral stiffness of a pneumatic tire has been assumed to be constant, regardless of material behaviour.2) Footprint is assumed to have a rectangular shape and pressure distributed in a parabola shape along the x-axis. 3) Tire friction model refers to Coulomb's Friction. Those 3 parts of the assumption do not represent the actual pneumatic tire properties and can be improved by theorems that have been created over many years.

From Chapter 4.2 through 4.6, the author proposes a method to improve the classical brush model in each parameter and also shows how each parameter affects the calculation result. In Chapter 4.1, explanation is given concerning the improvement of lateral stiffness for pneumatic tires that will refer to material behaviour. Chapter 4.2 and 4.3 will improve the footprint and pressure distribution shape to have better assumption. Chapter 4.4 and 4.5 will focus on the friction model of tire-road contact.

4.2 Material Properties

Tires are made from rubber that consists of Hyperelastic and Viscoelastic properties. Which means the stiffness of the tire should be nonlinear. But in the calculation is assumed that the lateral stiffness of the tire is constant.

Hyperelastic material can be explained in terms of strain energy (W) from the integration of strain energy density (U) in object volume ($\forall$). The term of strain energy density can be represented by many kinds of theorems. The theorem chosen for use in this research will refer to Yang's research [9]. Therefore, Yeoh's model will be used.

$$W = \int \sigma d\varepsilon = \int_{\forall} U d\forall \tag{4.1}$$

$$U = C_{10}\left(\bar{I}_1 - 3\right) + C_{20}\left(\bar{I}_1 - 3\right)^2 + C_{30}\left(\bar{I}_1 - 3\right)^3 \tag{4.2}$$

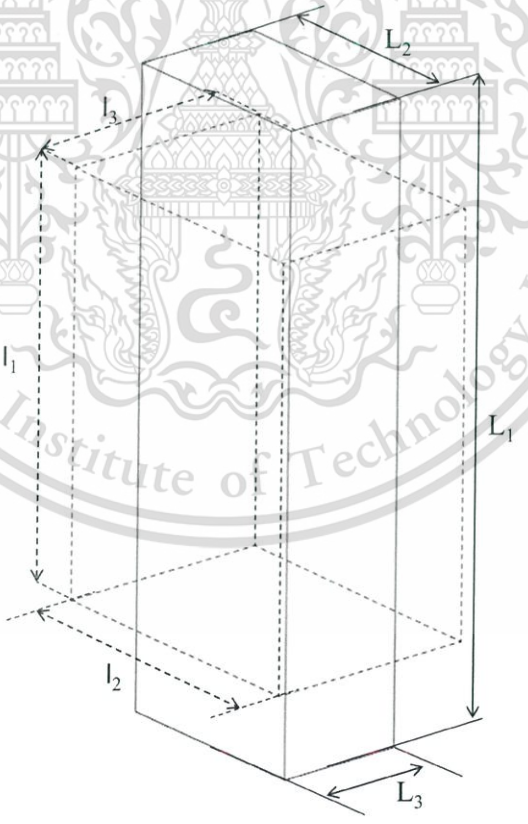

Figure 4.2 Specimen at unloaded (dash line) and loaded (solid line)

Yeoh's model has an advantage in the testing procedure because it requires only uni-axial tensile testing. From the testing result, nominal stress and nominal strain can be evaluated and plotted. From the nominal stress and nominal strain, the strain energy can be calculated from the trapezoid rule. Then, cure fitting can be done by choosing 3 points of data and solving from a linear equation.

$$\lambda_i = \frac{L_i}{l_i} = \frac{l_i + \Delta l_i}{l_i} \tag{4.3}$$

$$\lambda_i = 1 + \varepsilon_i \tag{4.4}$$

The stretch of material (λ_i) can be evaluated from Equation 4.4. Since the rubber can be assumed to be incompressible material, the volume of the specimen at load and unload will be equal. Rubber also has isotropic material, so the strain in both y-axis and z-axis are the same. Therefore, transverse strain can be evaluated from Equation 4.10.

$$l_1 l_2 l_3 = L_1 L_2 L_3 \tag{4.5}$$

$$\frac{l_2 l_3}{L_2 L_3} = \frac{L_1}{l_1} \tag{4.6}$$

$$\frac{1}{(1+\varepsilon_2)(1+\varepsilon_3)} = 1 + \varepsilon_1 \tag{4.7}$$

$$\varepsilon_2 = \varepsilon_3 \tag{4.8}$$

$$\frac{1}{(1+\varepsilon_2)^2} = 1 + \varepsilon_1 \tag{4.9}$$

$$\varepsilon_2 = \sqrt{\frac{1}{1+\varepsilon_1}} - 1 \tag{4.10}$$

Start with choosing 3 values of strain in the load-axis and evaluate transverse axis strain and stretch in every axis. Then, calculate the strain invariant from equation 4.11 and 4.12. Volumetric compression ratio (J) is equal to 1 because rubber can be assumed to be incompressible. By substituting $\bar{I}_1$ into Equation 4.2, this has to equal with the strain energy from the testing result, and the linear equation can be created.

$$\bar{\lambda}_i = J^{1/3}\lambda_i \tag{4.11}$$

$$\bar{I}_1 = \bar{\lambda}_1^2 + \bar{\lambda}_2^2 + \bar{\lambda}_3^2 \tag{4.12}$$

For example, choosing axial strain = 1, then the transverse strain will be $\frac{1}{\sqrt{2}} - 1$.

The first strain invariant is $4 + \left(\frac{1}{\sqrt{2}}\right)^2 + \left(\frac{1}{\sqrt{2}}\right)^2 = 5$. The testing result shows that total strain energy is equal to 305,672 Jules when strain equals 1. Equation 4.2 will give$305,672 = C_{10}(2)+C_{20}(2)^2+C_{30}(2)^3$ or $305,672 = C_{10}(2)+C_{20}(4)+C_{30}(8)$. Do this for strain = 0.46 and 0.68 will give invariant ~3.5 and 4, respectively. The other 2 equations will be $77,048 = C_{10}(0.5)+C_{20}(0.25)+C_{30}(0.125)$ and $146,465 = C_{10}+C_{20}+C_{30}$.

Solve the 3 linear equations for 3 unknown constants given as C_{10}, C_{20}, and C_{30} equal to 171,330 Pa, -43,980 Pa, and 17,370 Pa respectively.

Yang's research has also already done the testing and gives the coefficient. The calculation gives the constants, as shown in Table 4.1. The results may be a little bit different, but they give only slight differences in the stress-strain calculation. This error can occur if the strains that are chosen for use in the evaluation are different.

C10 (N/mm^2)	C20 (N/mm^2)	C30 (N/mm^2)
0.1714	-4.4041×10^{-2}	1.7383×10^{-2}

Table 4.1 Material properties of tire tread, Hyperelastic type, Yeoh Model **[9]**

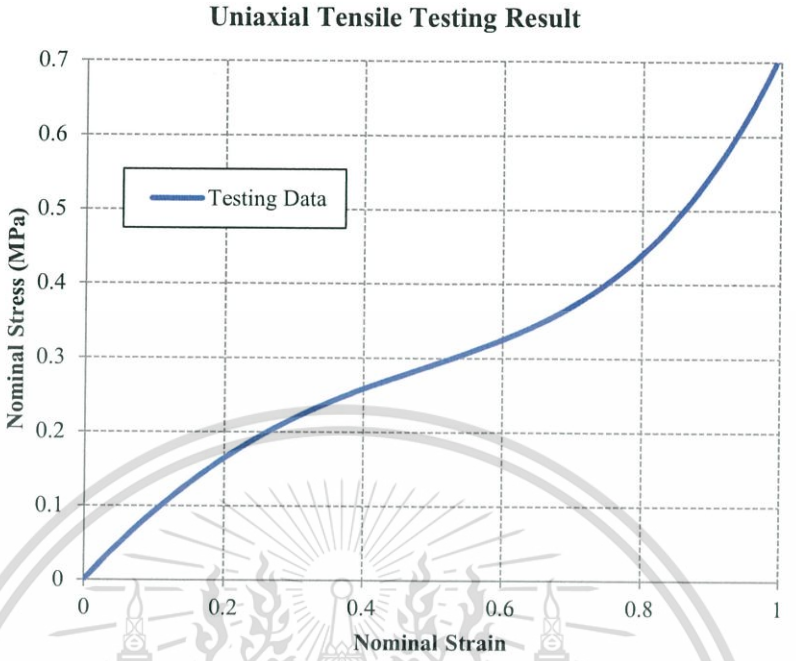

Figure 4.3 Uniaxial tensile test of Hyperelastic material

In the Brush Model, the tread elements are assumed to deform along the slip angle line. Therefore, the calculation can start from strain evaluation and substitute into Equation 4.10, 4.4, 4.12, and 4.2 to verify total strain energy in each tread element. Afterward, use the differential to evaluate the Nominal Stress and Elastic Modulus of each tread element. Then, use the Shear Force evaluation, Equation (4.13), to verify the Lateral Stiffness of the tread element.

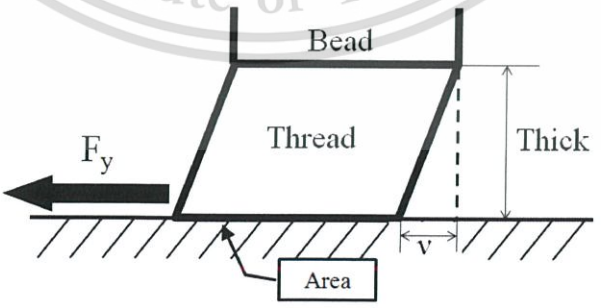

Figure 4.4 Lateral stiffness of thread

$$c_{py} = \frac{F_y}{v \cdot Area} = \frac{E}{3 \cdot Thick} \tag{4.13}$$

Equation 3.1 is done on the assumption that Lateral Stiffness is constant. Therefore, the calculation for Nonlinear Lateral Stiffness needs to rearrange the equation since Lateral Stiffness is a function of tire tread deformation. The equation for total Lateral Force should be written as Equation 4.14. Lateral Force in each tread element (F_v) is defined by Equation 4.15. Self-Aligning Torque will be evaluated from Equation 4.16.

$$F_y = b\int_0^l F_v(x) c_{py}(\upsilon(x))dx \tag{4.14}$$

$$F_v = \begin{cases} c_{py}(x) \cdot x \cdot \tan\alpha & \cdots AdhesionZone \\ \mu \cdot \left[\frac{4P_m}{l^2} \cdot \left(\frac{l}{2} - x\right)^2 + P_m\right] & \cdots SlipZone \end{cases} \tag{4.15}$$

$$M_z = b\int_0^l F_v(x) \cdot c_{py}(x) \cdot x_t dx \tag{4.16}$$

Other than Hyperelastic, the rubber also consists of Viscoelastic properties. Since the calculation uses a quasi-static assumption, Viscoelastic will not be included in the calculation. By excluding Viscoelastic, the calculation model will not be complex because it is independent of time.

The calculation takes place by substituting the C_{py} with 1) Constant calculated from average elastic modulus at ε=0 to 1. 2) Constant calculated from average elastic modulus at ε=0 to 0.07. 3) Elastic modulus as a function of tread deformation. The results show that constant lateral stiffness at low strain and nonlinear lateral stiffness model give similar results close to the FEA calculation result (see Figure 4.5).

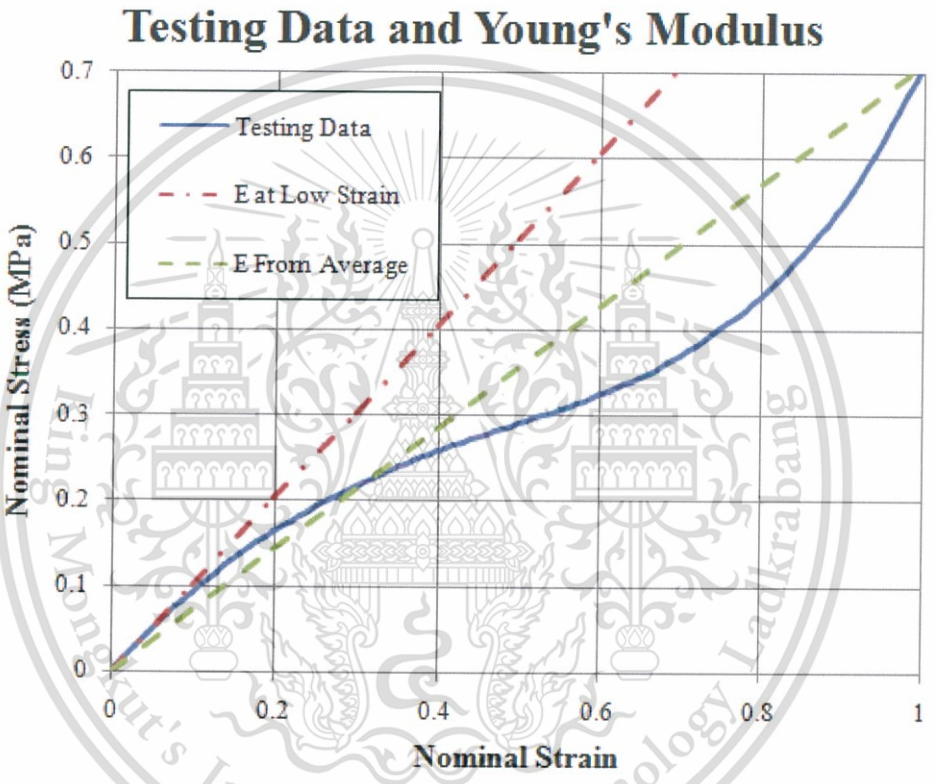

Figure 4.5 Linear assumption from nonlinear testing result

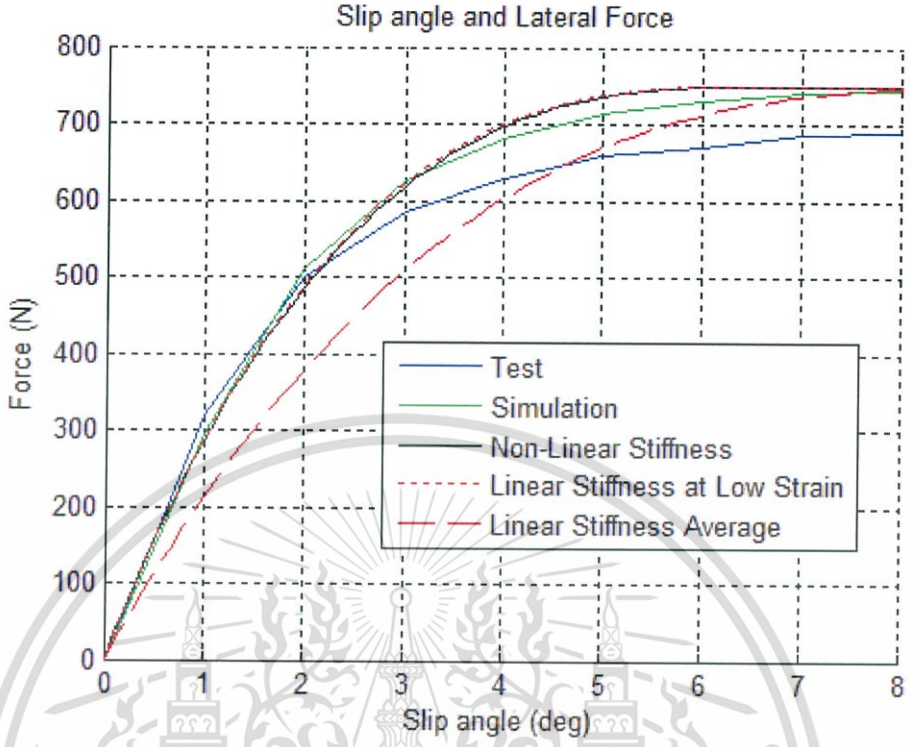

Figure 4.6 Comparison of linear and nonlinear stiffness

The reason that the Hyperelastic properties give a similar result as linear elastic in the calculation is because the brush model is concerned only with the deformation of tread during slip angle occurrence. The slip angle is only 8 degrees and the contact length and width are75.4 mm and 151.4 mm, respectively. The strain that occurred in the tread was around 0.07. Therefore, the usage average elastic modulus at ε=0 to 0.07 is acceptable since the Hyperelastic effect occurred after strain higher than 0.2. The Proposed Tire Model will exclude the nonlinear lateral stiffness in the case that tire tread has low strain to reduce complexity and calculation time. However, nonlinear modeling of lateral stiffness will be included if the tire tread has high strain (in this case more than 0.2). The criteria strongly depend on material properties and footprint shape.

4.3 Contact Area

As mentioned in Chapter 3, the classical brush model calculation was done on the assumption that the footprint shape is rectangular. In an actual tire, however, the footprint has various shapes depending on tread, load, tire size and structure. To keep the calculation simple, the ellipse shape has better similarity to the actual footprint. Therefore, the calculations will be done referring to the elliptical shape of the footprint.

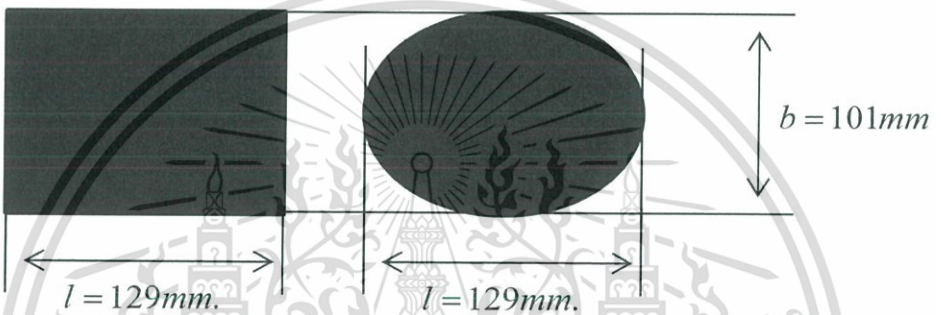

Figure 4.7 Footprint shape change from rectangle to ellipse

The pressure distribution in Equation (2.8) has to change since the pressure is varied on both x and y axis. Therefore, Equations (2.9) and (2.12) have to change also. The pressure distribution has a parabola shape when projected in both x and y axis. Equation (4.17) will be used in this case. However, the equation can give negative values outside the contact zone and reach false calculation. Therefore, a negative result will not be included in the tire force calculation.

$$P(x,y) = P_m - P_m\left[\left(\frac{x - l/2}{l/2}\right)^2 + \left(\frac{y}{b/2}\right)^2\right] \qquad (4.17)$$

When substituting (x,y) coordinates outside the footprint of the tire, the result from Equation (4.17) will be less than 0. The coding process can use if-else logic to change the negative data into 0. P_m also needs to be re-calculated since total pressure in the footprint area has to equal vertical load (F_z).

$$F_z = \int_0^l \int_{-b/2}^{b/2} P(x,y)\,dy\,dx \qquad (4.18)$$

From Equation (4.17) and (4.18), the integration is complicated since the equation (4.17) consists of 2 variable parameters. Therefore, integration needs to be done with multi-variables. Since the area of the ellipse in each P-axis is easier to define, Equation (4.19) will be used instead. After carrying out some mathematical calculations, P_m will be calculated using Equation (4.20).

$$F_z = \int_0^{P_m} Area(P)\,dP = \frac{\pi \cdot l \cdot b \cdot P_m}{8} \qquad (4.19)$$

$$P_m = \frac{8F_z}{\pi \cdot l \cdot b} \qquad (4.20)$$

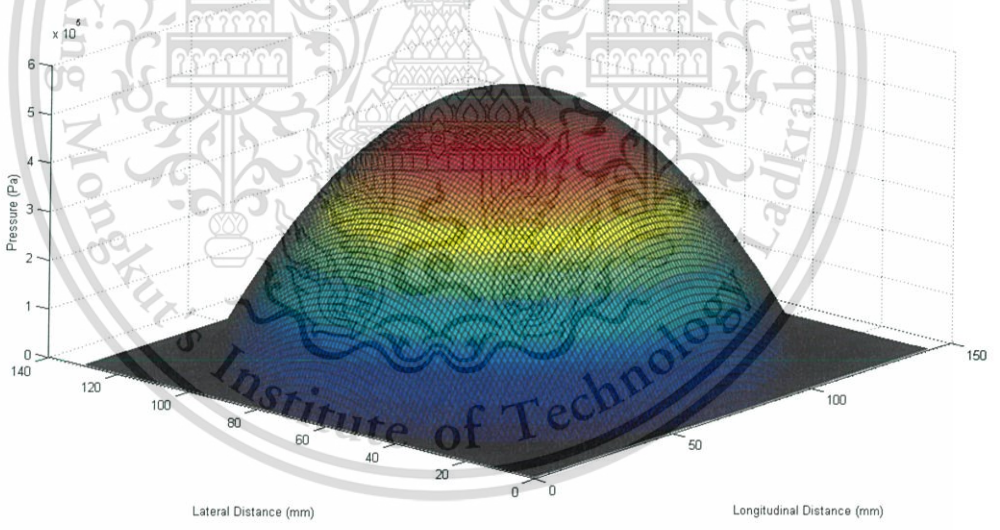

Figure 4.8 Pressure distribution in the footprint with ellipse shape

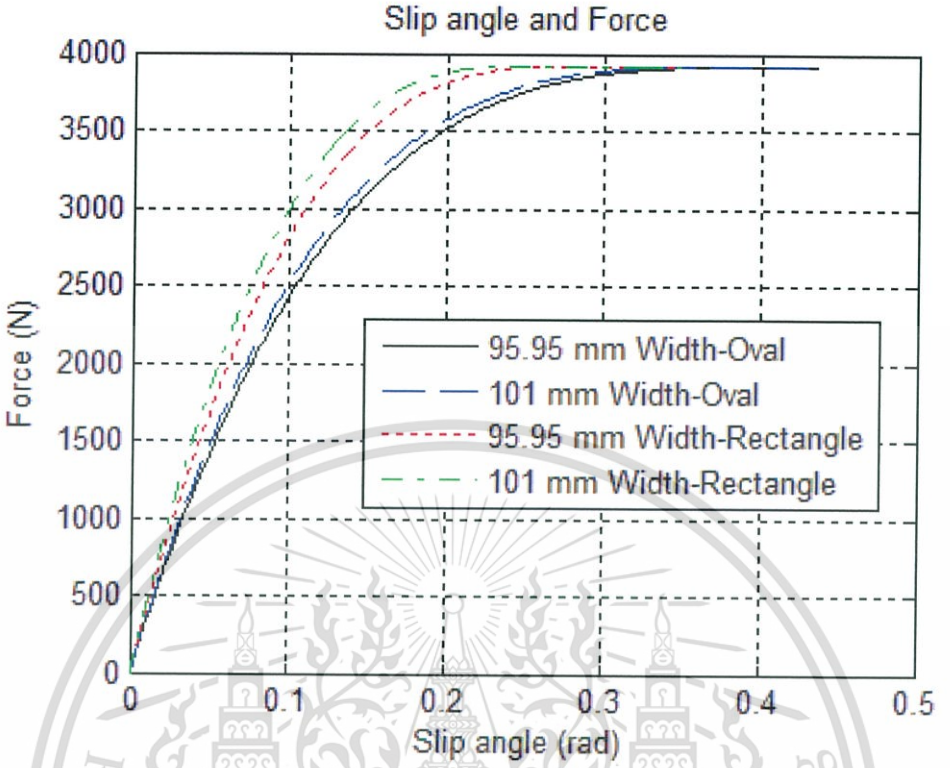

Figure 4.9 Calculation result of rectangular and ellipse footprint shape

The comparison of slip-force graph for ellipse and rectangle shape of contact area with different width is shown in Figure 4.9. The results show that the maximum lateral forces are all the same. Only the cornering stiffness is different. This means improvement in the contact area can affect cornering stiffness, but not affect maximum lateral force.

In real cases, pressure distribution in the footprint area can be analyzed by using a testing machine and/or image processing. In the case that the facility is not accessible, the FEA is an acceptable alternative method to evaluate the pressure distribution. The FEA calculation time for footprint analysis is not long, but CAD modeling is complicate.

4.4 Tilting Pressure Distribution

From the simulation result in Yang's research and discussion in BNJ Persson's research, the suggestion is that pressure distribution during cornering is tilted in the lateral axis. When considering Figure 2.7 in pure side slip case, self-aligning torque is calculated from a summation of the product for lateral force in each tread element multiplied by the distance between tread element and rotational axis. Since the element that has the same x-position will have the same distance from the rotational axis, the force of each element that has the same x-position can be summed before multiplying by the distance. Therefore, the lateral force in each tread element can be summed along the y-axis before multiplying by distance. This means the pressure tilting in the y-axis will give the same self-aligning torque as normal pressure distribution.

From Equation 4.17, the tilting pressure distribution can be done by changing the centre of the ellipse along the y-axis when P is higher. This means the bracket (y) has to change into $\left(y + \frac{Pb}{P_m 4}\right)$, and then solve the equation for P by using a quadratic formula.

The calculation result shows that tilting pressure distribution along the y-axis does not give a different result for lateral force or self-aligning torque.

Pressure distribution tilting along the x-axis can be done in the same way as tilting along the y-axis. Further, it gives different self-aligning torque. However, the calculation done on the assumption that the tire is in a free-rolling state means the pressure distribution does not tilt along the x-axis. If the pressure tilting is along the x-axis, rolling resistance occurs.

4.5 Static-Kinetic Friction

In classical physics [21], the friction coefficient when an object does not slip on surface, so-called "Static Friction," normally generates higher friction force. After an object starts to slip, the fiction coefficient will decrease to a specific value, so-called

"Kinetic Friction Coefficient." Majorly, the Kinetic Friction Coefficient value is lower than the Static Friction Coefficient.

By applying the Kinetic Friction Coefficient in the calculation, the result shows that different tire widths can generate different lateral forces. The calculation has been done with a rectangular footprint. The changing friction coefficient instantly makes the graph uneven. In the calculation for 10% difference, the maximum lateral force difference is only 0.01%.

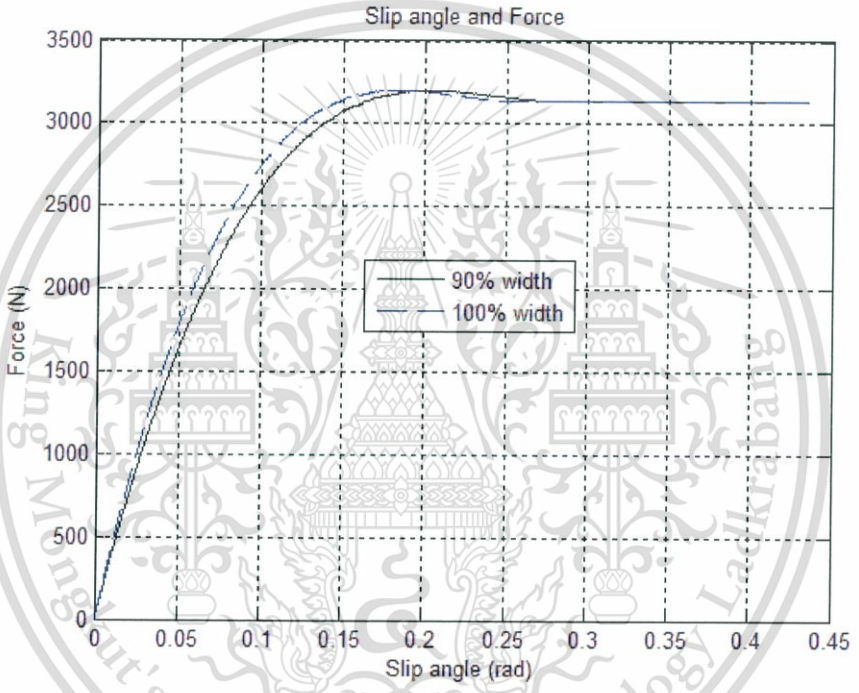

Figure 4.10 Static-Dynamic Friction Model result

From the calculation result, this is the first time that a contact shape has an effect with the maximum lateral force. At this point, the author strongly suggests that the friction model must be improved. Since the model used in this part is rough and does not have enough explanation concerning rubber-like material, further research finally meets with BNJ Persson's work in "Flash Temperature" and "Cold-Hot Friction Law".

4.6 Cold-Hot Friction Law

Referring to [5], "Cold-Hot Friction Law" is easier to use and gives similar results as the full temperature history model. It consists of 1 main equation, Equation (4.21), and data of μ_{cold} and μ_{hot} as functions of ambient temperature and vehicle speed.

$$\mu_{eff}(t) = \mu_{cold}(V(t),T_0)e^{-r(t)/r_0} + \mu_{hot}(V(t),T_0)[1-e^{-r(t)/r_0}] \quad (4.21)$$

The calculation for effective friction coefficient is done by setting the ambient temperature and velocity as constant, then finding the cold and hot friction coefficient. The macro-asperity contact region diameter (r_0) is assumed to be constant at 10 mm, as suggested in [5].

For the slip distance r(t), slip distance can be evaluated by a function of position x and y axis since the brush model calculation is done on the assumption of steady-state slip. Then r(t) will be transformed to r(x,y) by evaluating from the figure below.

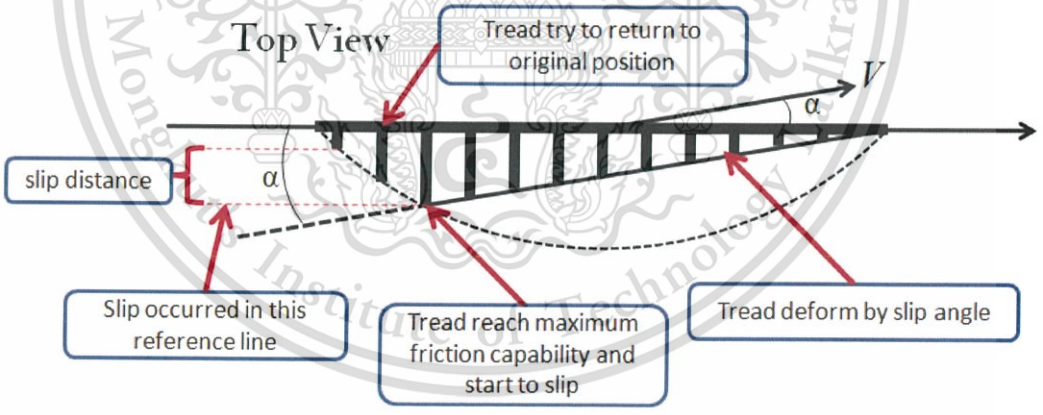

Figure 4.11 Defining the slip distance for steady state slip condition

Since the calculation is done on steady-state slip and pure side slip, the tire will roll continuously and tread element will not slip in the x-axis. Therefore, the tread elements are moving in x-direction by the rolling of the tire. When the tread element

reaches the maximum deformation capability, it will start to slide back to the wheel plane. Because it is pure side slip, the tread element will not slip in x-direction. Therefore, sliding direction will occur in the y-direction only. If the tread element position after slip has been evaluated, the slip distance can be evaluated as well by Equation (4.22).

$$r(t) = r(x, y) = v(x, y) - v_{ref} \tag{4.22}$$

$$v(x, y) = \frac{\mu_{cold} P(x, y)}{c_{py}} \tag{4.23}$$

$$r(t) = r(x, y) = \frac{\mu_{cold} P(x, y)}{c_{py}} - v_{ref} \tag{4.24}$$

Start from defining the position that the tread element starts to slip, v_{ref} and calculate for actual tread element position after slip, v(x,y). Since the effect of Viscoelastic has been neglected, the tread element will slip until it reaches the maximum capability at that position. Afterward, v(x,y) can be evaluated from force balance between Adhesive Zone and Slip Zone to achieve Equation (4.23). Then, substitute into Equation (4.22) to get Equation (4.24). Therefore, $\mu_{eff}(t)$ (time-based function) can be transformed into $\mu_{eff}(x,y)$ (coordinate-based function). Since the calculation is done in steady-state slip and pure side slip, the μ_{cold} and μ_{hot} are constant. Equation (4.21) can be simplified into Equation (4.25), as shown below:

$$\mu_{eff}(x, y) = \mu_{cold} e^{-r(x,y)/r_0} + \mu_{hot}[1 - e^{-r(x,y)/r_0}] \tag{4.25}$$

The relationship between slip distance and effective friction coefficient is shows in Figure 4.12. At higher slip distance, the effective friction coefficient is converging to μ_{hot}. Therefore, it can be evaluated from friction coefficient that occurred at full-slip.

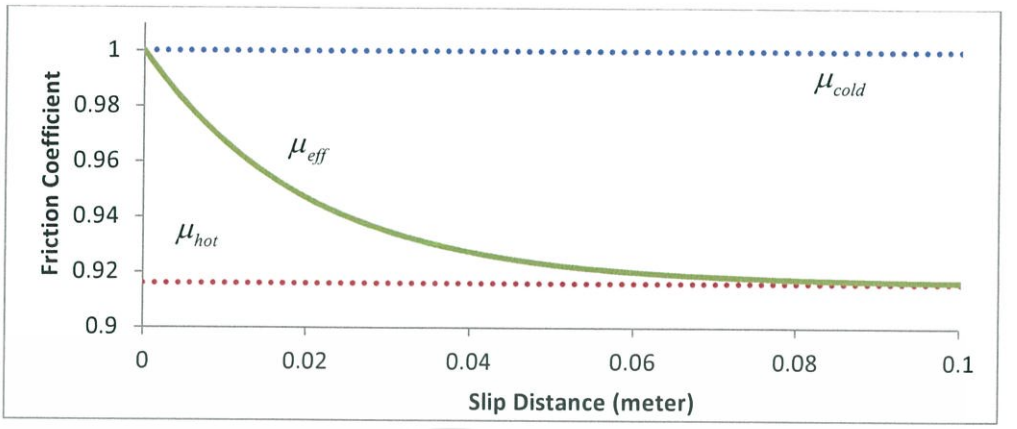

Figure 4.12 Graph of relationship between slip distance and friction coefficient.

4.7 Proposed Tire Model

From the theorem in 4.2 to 4.6, the Proposed Tire Model will consist of Nonlinear Lateral Stiffness, Ellipse Footprint Shape, and Cold-Hot Friction Law. The overall calculation procedure is shown in Figure 4.12.

Figure 4.13 Flowchart of Proposed Tire Model

CHAPTER 5

VALIDATION AND CALCULATION RESULTS

The validations refer to 2 sources: 1) Lecture Documents 2) Yang's Research throughout Chapter 5.1 and 5.2, respectively. Chapter 5.3 will bring the Proposed Model to apply with truck tires for both normal dual tires and WBS tires. In Chapter 5.4 will roughly calculate for vehicle dynamics of the truck. The results are discussed in Chapter 5.5, while conclusions are given in Chapter 6.

5.1 Lecturing Document

In July 2015, Dr. Sunao gave a lecture on "Basic/Advanced Engineering for Automotive Course" organised by JSAE and NSTDA. The document used for lecturing has testing results and classical brush model calculation with all necessary tire data. Therefore, this document can be used as validation.

The tire has a footprint 129 mm long and 101 mm wide at 3920 N of vertical load. It has a friction coefficient equal to 1 and lateral stiffness of 53.6 N/mm^2. The calculation results show that they converge to 3920 N at full-slip, as expected. Furthermore, their maximum lateral force is still the same after applying this calculation to find the force generated from similar tires that have different widths (b=70.7, 101, 131.3 mm).

The calculation of classic brush model was done with a rectangular footprint. As mentioned in 2.2, however, the footprints are majorly similar to an ellipse shape. Since the document doesn't give the footprint testing result, the ellipse shape will be done in 2 methods: 1) same length 2) same area. Each method gives different results, as shown in each section.

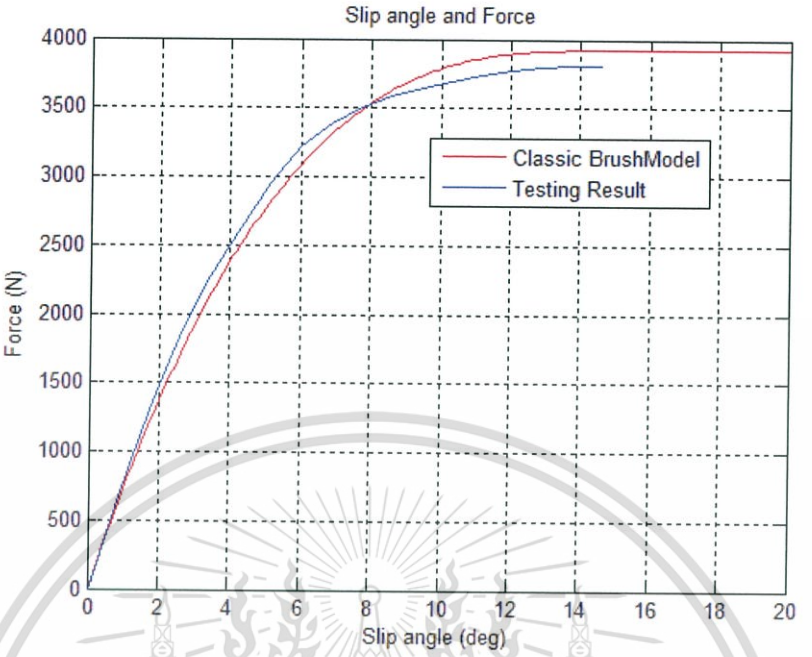

Figure 5.1 Classic Brush Model that used in lecture document

5.1.1. Ellipse Shape at Same Length and Width

By the assumption that contact shape has the same length and width but comes in an ellipse shape, the footprint should look like that in Figure 33. The other parameters remain the same as represented in the document. For friction coefficient, μ_{cold} will equal 1 the same as the original friction coefficient. For μ_{hot} has defined from testing result at full-slip. At full-slip, tire generates 3,810 N. of lateral force. Therefore friction coefficient at full-slip should be equal to 0.972. The parameters used in the calculation are shown in Table 2.

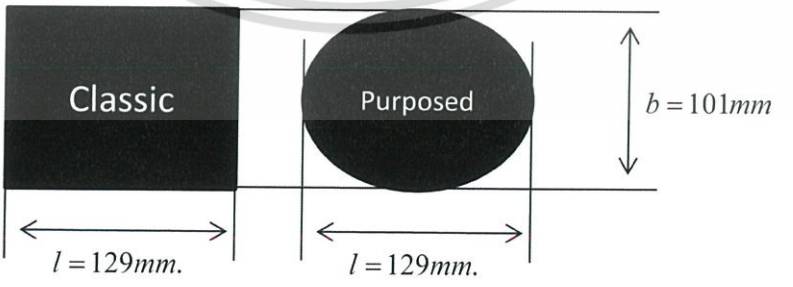

Figure 5.2 Contact shapes of 2 different methods, same length and width.

Contact Shape	Contact Length, l (m)	Contact Width, b (m)	c_{py} (N/m)	Vertical Load, F_z (N)	μ_{cold}	μ_{hot}	r_0 (m)
Ellipse	0.129	0.101	53.6×10^6	3,920	1	0.972	0.01

Table 5.1 Parameters for calculation in lecture, same length

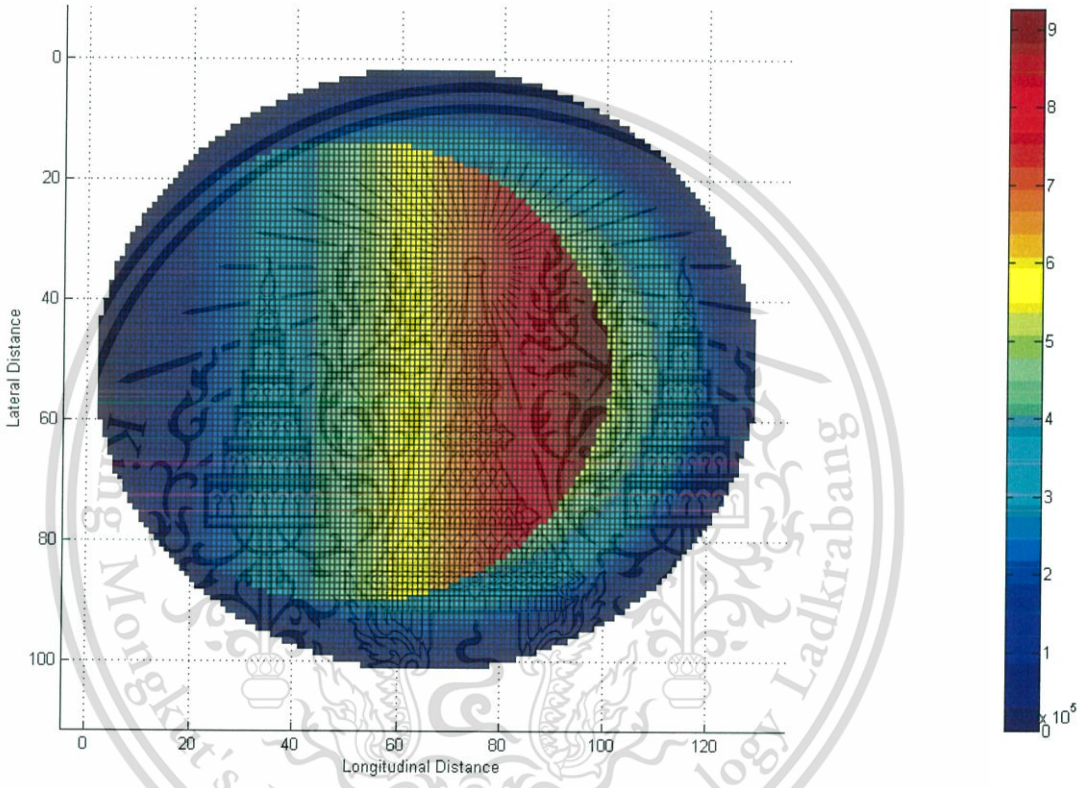

Figure 5.3 Lateral force generated by thread element

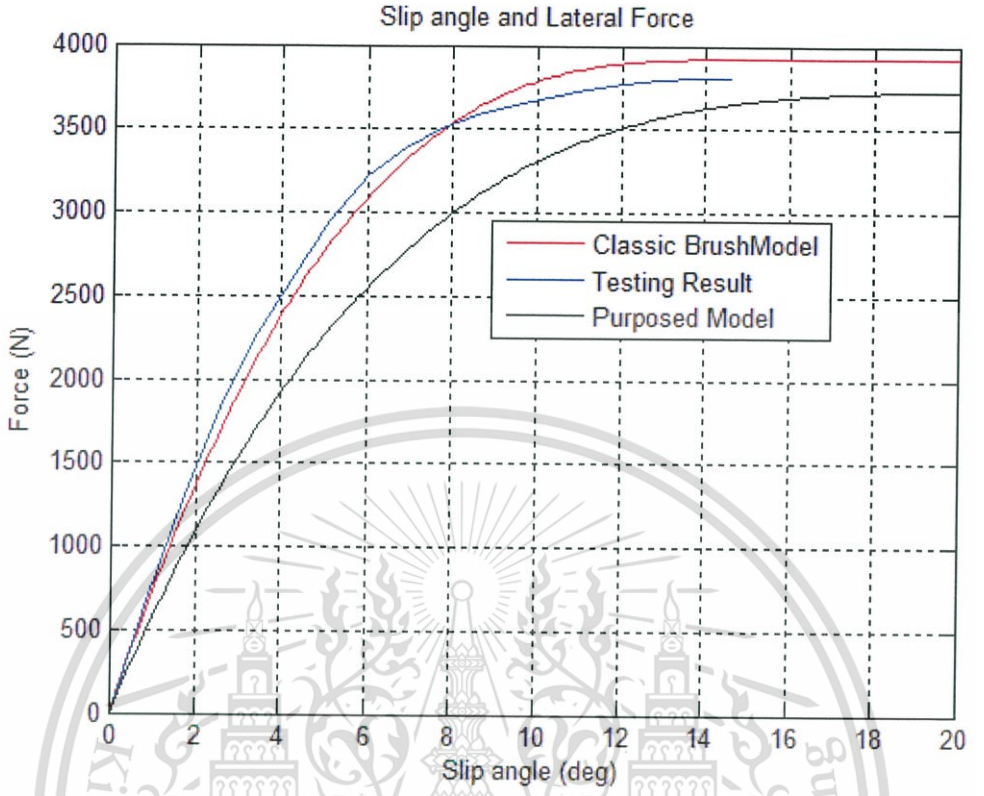

Figure 5.4 Calculation result in lecture at same contact length and width

The calculation result shows that this assumption gives unacceptable results. The lateral force at full slip may be similar to the testing result, but the cornering stiffness is far lower than the testing result. Full-slip also occurred at higher slip angle. This kind of effect comes from a contact area that is reduced because the contact shape changes into an ellipse by maintain contact length and width, as shown in Figure 5.2.

5.1.2. Ellipse Shape at Same Area

The calculation is done again, but with changes in contact length and width to get the same contact area as a rectangular shape while maintaining the aspect ratio of the contact shape. After carrying out some calculations, the contact length and width changed to 0.14556 and 0.11397 metres, respectively. The other parameters are maintained.

Contact Shape	Contact Length, l (m)	Contact Width, b (m)	c_{py} (N/m)	Vertical Load, F_z (N)	μ_{cold}	μ_{hot}	r_0 (m)
Ellipse	0.14556	0.11397	53.6×10^6	3,920	1	0.972	0.01

Table 5.2 Parameters for calculation in lecture, same area

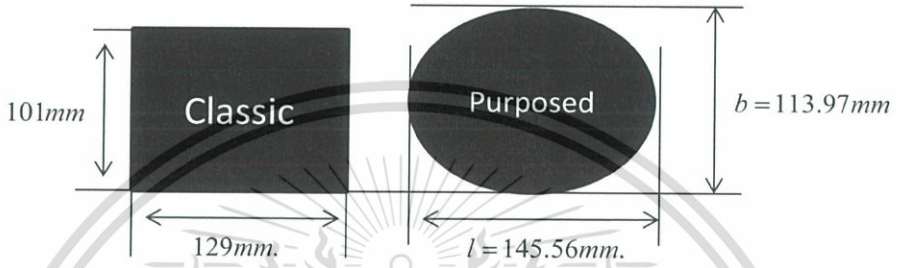

Figure 5.5 Contact shapes of 2 different methods, adjusted size of ellipse to maintain area.

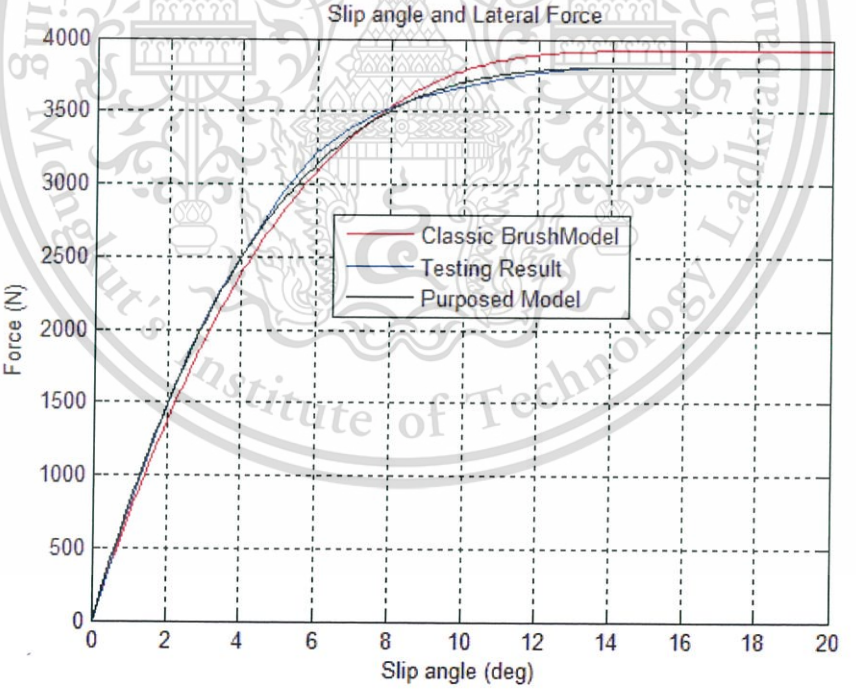

Figure 5.6 Calculation result in lecture at same contact area

5.2 Yang's Research

The validation is referred to Yang's work [5] for both material properties and testing results. Material properties are shown in Table 4.1 and tread thickness is 5 mm. Therefore, Nonlinear Lateral Stiffness is able to be evaluated. From testing at 750 N. of vertical load, the photo of the footprint is 340 pixels wide and 170 pixels long in the shape of a rounded rectangle with 9000 mm^2 of area. Since the assumption of pressure distributed in a rectangular shape is not accurate, the ellipse shape will be used in the calculation instead. By maintaining the aspect ratio and area of the footprint, the calculation for an ellipse footprint shape is151.4 mm wide and 75.4 mm long.

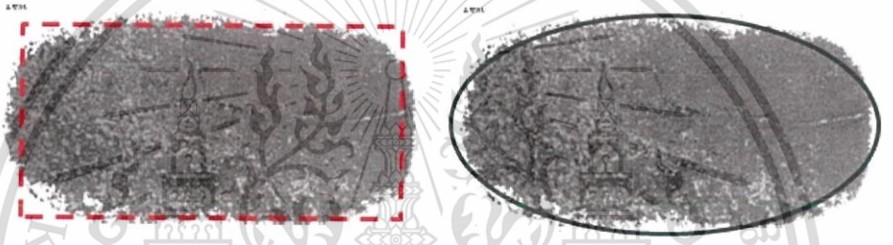

Figure 5.7 Footprint shape assumption [9]

From elastomer tensile testing to get data for the Hyperelastic material, the elastic modulus is 1.013 MPa. Tread thickness is 5 mm. Therefore, lateral stiffness is 63.69 N/cm3. For the friction coefficient, the research specified as 1 and is constant along the calculation. To apply with Cold-Hot Friction Law, however, μ_{cold} and μ_{hot} must be evaluated. For μ_{cold}, it can be assumed as 1. μ_{hot} is calculated from the lateral force at full slip. Therefore, μ_{hot} is equal to 0.88.

Contact Shape	Contact Length, l (m)	Contact Width, b (m)	Vertical Load, F_z (N)	μ_{cold}	μ_{hot}	r_0 (m)
Ellipse	0.0754	0.1514	750	1	0.88	0.01

Table 5.3 Parameters for calculation in Yang's work at 750 N

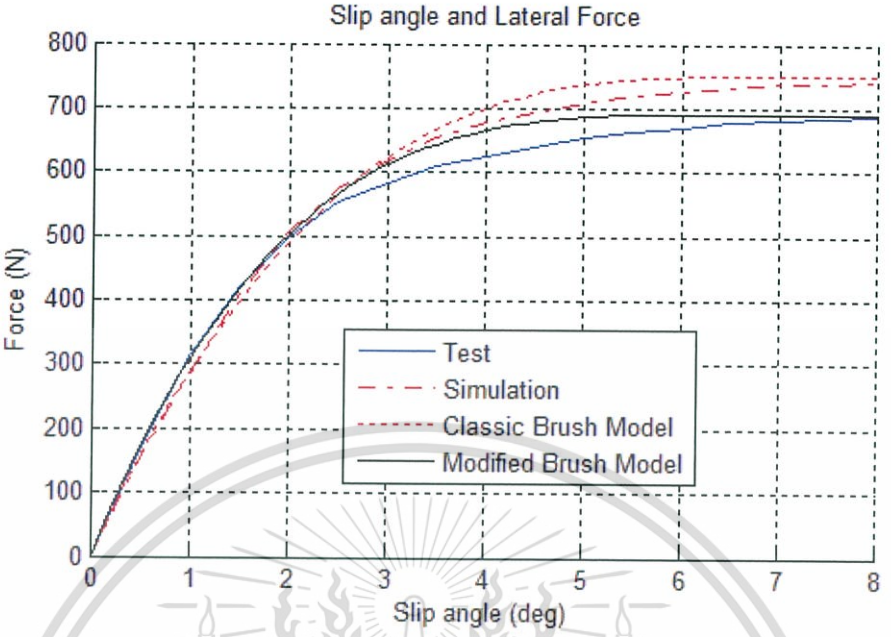

Figure 5.8 Comparison between testing, FEA, Classic Model, and Proposed Model

The photo of footprint testing at 500 N and 1000 N vertical load does not represent as Yang's research [9], but is shown as a graph of Contact Area-Vertical Load instead. The calculation for 500 N and 1000 N will be done on the assumption that the footprint has maintained its aspect ratio and increased only in size. Therefore, the contact shape can be calculated by the rule of scaling.

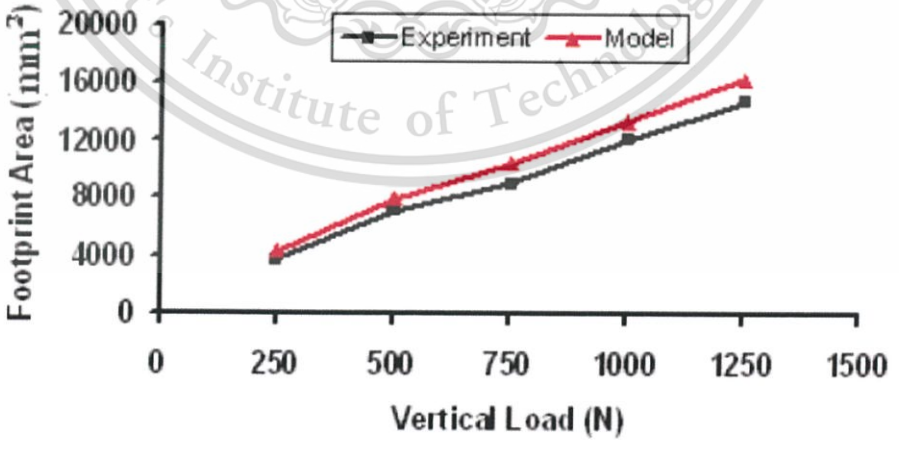

Figure 5.9 Contact area with respect to vertical load **[9]**

Contact Shape	Contact Length, l (m)	Contact Width, b (m)	Vertical Load, F_z (N)	μ_{cold}	μ_{hot}	r_0 (m)
Ellipse	0.0665	0.1335	500	1	0.88	0.01
Ellipse	0.0871	0.1748	1,000	1	0.88	0.01

Table 5.4 Parameters for calculation in Yang's work at 500 and 1,000 N

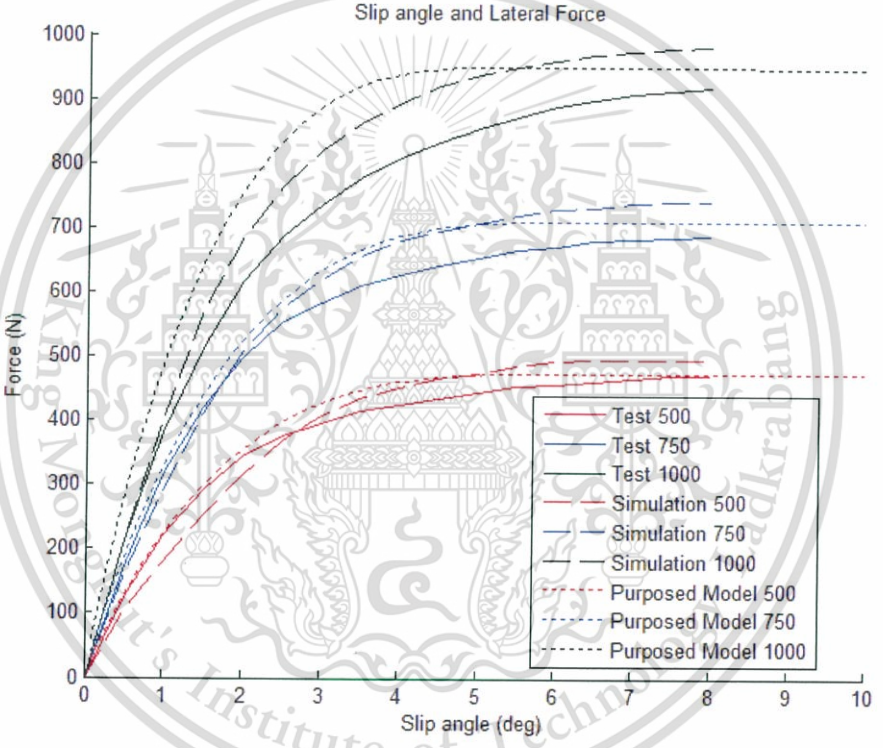

Figure 5.10 Calculation Result

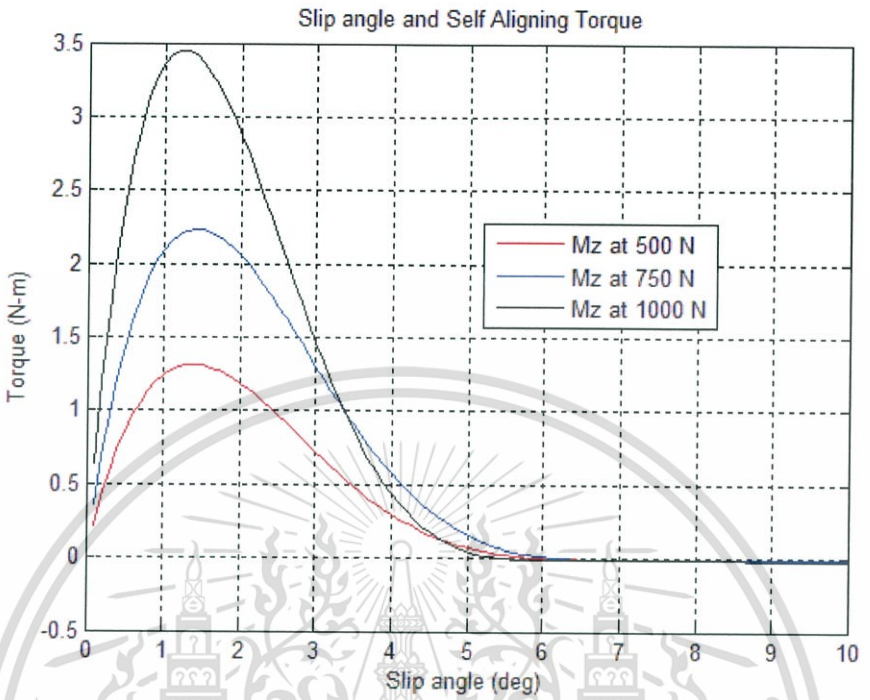

Figure 5.11 Calculation Result

5.3 Truck Tires Calculations

The tires that use in comparison are Michelin 11 R 22.5 XTE 2 TL 142/142 J (normal tire) and Michelin 455/55 R 22.5 X One XTE LRL (WBS tire). Michelin Siam Co., Ltd. provided some technical data for this research. The data does not contain the pressure distribution or the picture of footprint. The technical data contain only total area, contact length, contact width, and vertical load. The data will not show in this research since they are all confidential data of the company. The material properties and fiction properties does not contain in their data. But the tires are made of same material; therefore the material and friction properties are control parameters. Even in the case that data does not provided, those properties can be assign by same input is enough to observe the effect of tire width.

The calculation for WBS tire can be use the Proposed Model directly since the calculation parameters are provided. The vertical load that used for the calculation is 50,000 N (~5 tons) refer to weight index of the tire.

For normal dual tire, the calculation cannot directly apply into Proposed Model. Because the calculation for normal dual tire has 2 separated contact area. Consider in figure 5.10, lateral force that generated by dual tire is sum of lateral force in each tire. Since the calculation done on free-rolling and steady-state cornering, the pressure distribution in each tire can assumed to equal. Therefore the lateral force in each tire will be equal; the total later force will be 2 times of lateral force in each normal tire.

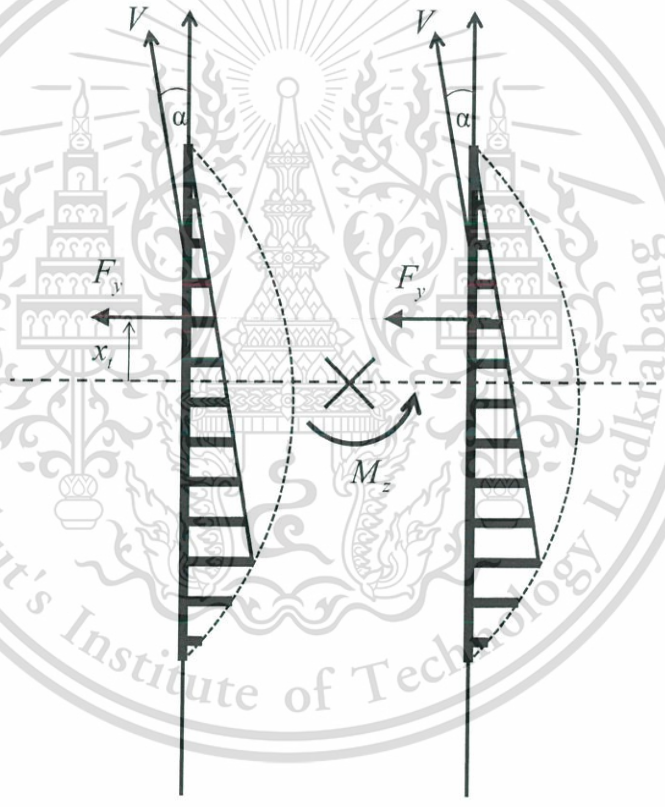

Figure 5.12 Schematic diagram of F_y and M_z analysis for dual tire

Self-Aligning torque can calculate from summation of torque in each tire. The calculation can be done with equation 5.2.

$$M_z = 2F_y x_t \tag{5.1}$$

$$M_z = 2b\int_0^l c_{py} F_v x_t dx \tag{5.2}$$

The calculation result for lateral force is show in figure 5.11 and for self-aligning torque is show in figure 5.12.

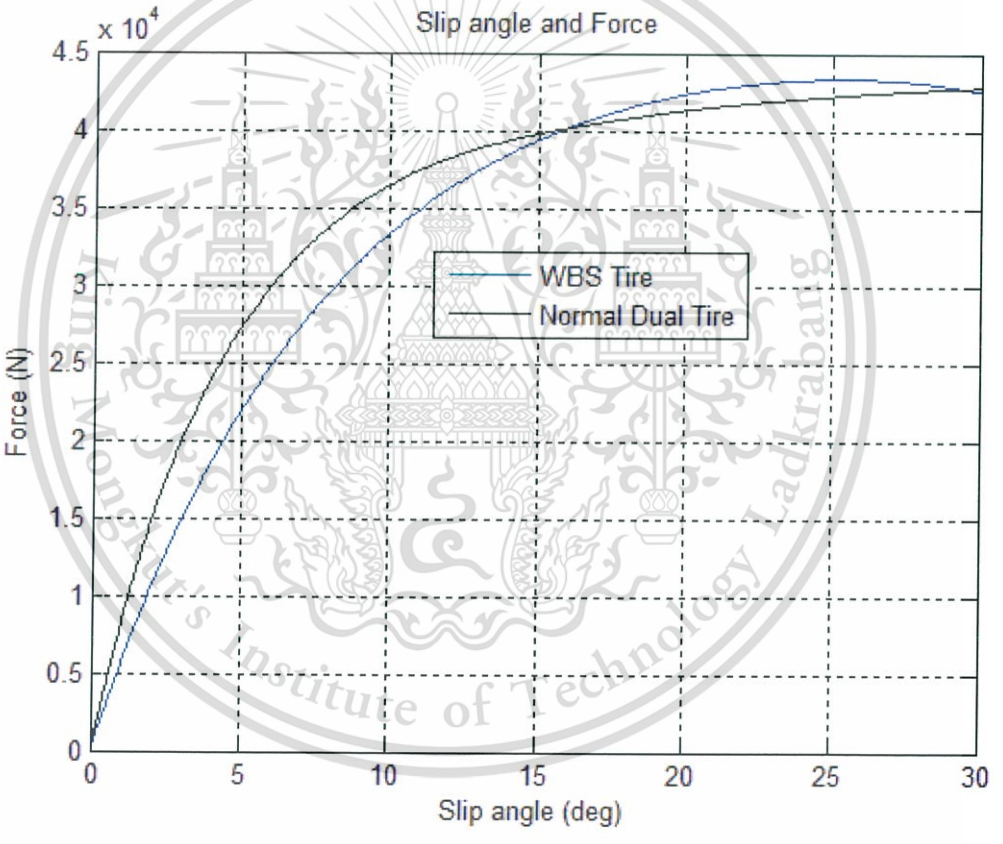

Figure 5.13 Calculation Result comparison between dual tire and WBS tire

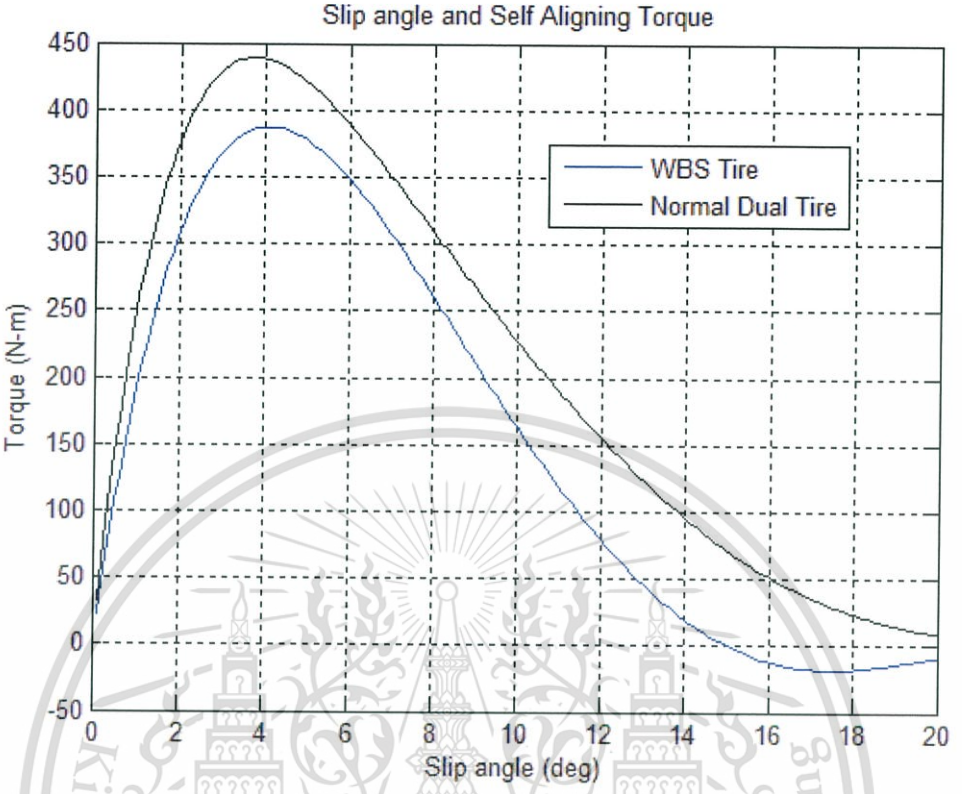

Figure 5.14 Calculation result comparison between dual tire and WBS tire

5.4 Vehicle Dynamics Comparison

From the research, the WBS tires are mostly used in long haul driving because it gives most efficient way for fuel economy. Therefore, the Vehicle Dynamics evaluation will be refer to the truck trailer configuration.

From the suggestion in "Race Car Vehicle Dynamics" [11], the evaluation of skid-pad cornering is enough to observe the vehicle cornering performance. The skid-pad course is the steady-state cornering, i.e. constant longitudinal speed and constant cornering radius. The evaluation will use bicycle model at low-speed cornering since the truck trailer majorly cornering at low speed.

From the configuration of the trucks, by merge the rear wheels into 1 single wheel and merge front wheels into 1 single wheel, the evaluation can be done by bicycle model. See figure 5.15.

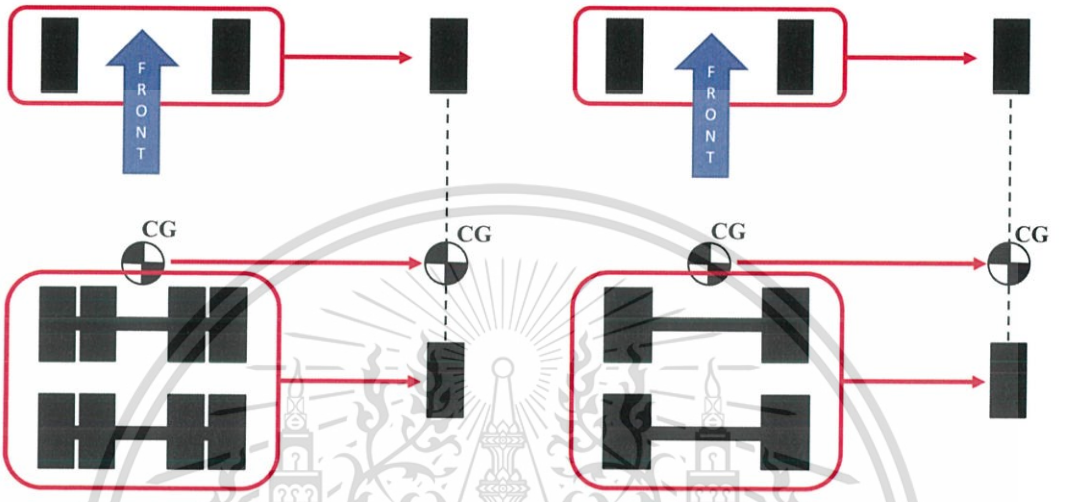

Figure 5.15 Simplify truck model into bicycle model, left stands for normal dual tire, right stands for WBS tire.

The steady-state cornering evaluation for bicycle model can be done from evaluation of velocity, slip angle, acceleration, and force balance.

According to figure 5.16, start with vehicle velocity and yaw rate at CG point, the actual velocity of the wheels at their center can now be evaluated from equation 5.3 to 5.6. Then slip angle of each tires can be evaluate from equation 5.7 to 5.9.

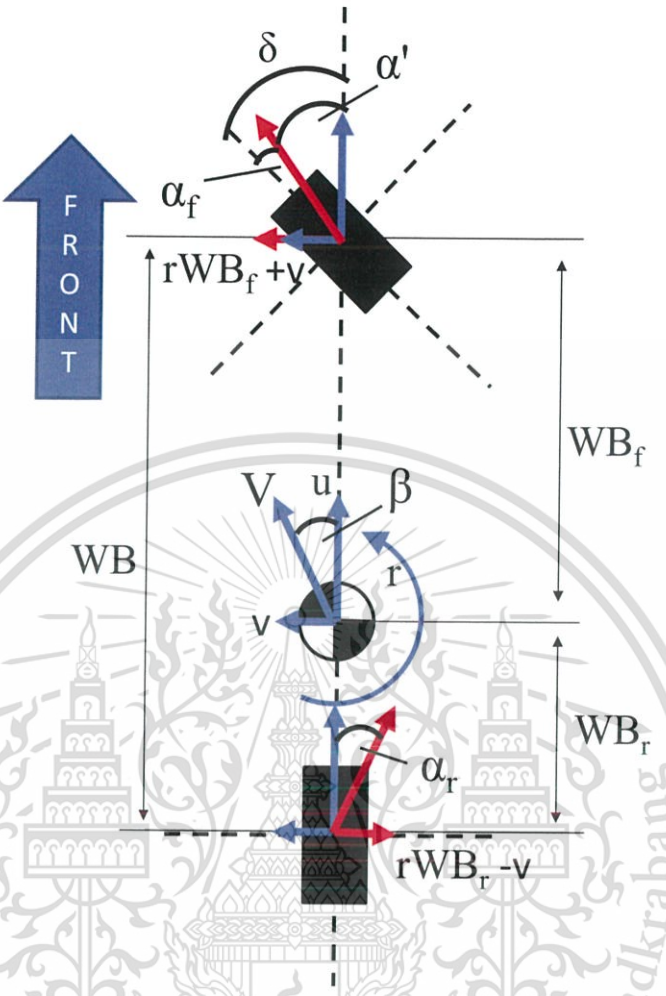

Figure 5.16 Velocity and Slip Angle of the bicycle model.

$$V_{fy} = r \cdot WB_f + \mathrm{v} \tag{5.3}$$

$$\vec{V}_f = \vec{u} + \overrightarrow{V_{fy}} \tag{5.4}$$

$$V_{ry} = r \cdot WB_r - \mathrm{v} \tag{5.5}$$

$$\vec{V}_r = \vec{u} + \overrightarrow{V_{ry}} \tag{5.6}$$

$$\alpha' = \arctan\left(V_{fy}/u\right) \tag{5.7}$$

$$\alpha_f = \delta - \alpha' \tag{5.8}$$

$$\alpha_r = \arctan\left(V_{ry}/u\right) \tag{5.9}$$

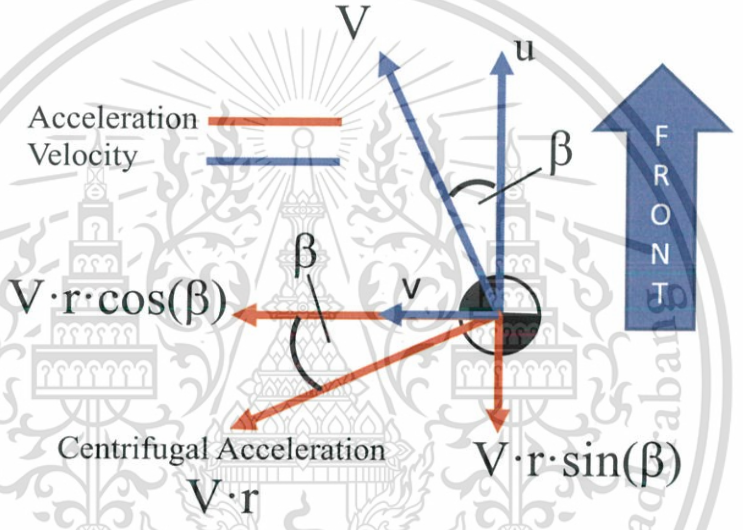

Figure 5.17 Acceleration at CG point.

From figure 5.17, evaluate the centrifugal acceleration of CG point. Then find the component in x and y direction. The total acceleration in each axis now able to evaluated from equation 5.10 and 5.11.

$$a_x = \dot{u} - \left(V \cdot r \cdot \sin(\beta)\right) \tag{5.10}$$

$$a_y = \dot{v} + \left(V \cdot r \cdot \sin(\beta)\right) \tag{5.11}$$

From the force balance and the moment balance of the whole vehicle, the equation 5.12 to 5.14 can be created.

$$F_{Vx} = m\left[\dot{u} - \left(V \cdot r \cdot \sin(\beta)\right)\right] \quad (5.12)$$

$$F_{Vy} = m\left[\dot{v} + \left(V \cdot r \cdot \sin(\beta)\right)\right] \quad (5.13)$$

$$M_{Vz} = J \cdot \dot{r} \quad (5.14)$$

By using the assumption for constant longitudinal speed, small steering angle, small vehicle side-slip angle, the equation 5.12 to 5.14 can be simplified into equation 5.15 to 5.17.

$$F_{Vx} = 0 \quad (5.15)$$

$$F_{Vy} = mV\left(\dot{\beta} + r\right) = F_{fy} + F_{ry} \quad (5.16)$$

$$M_{Vz} = J \cdot \dot{r} = WB_f \cdot F_{fy} + WB_r \cdot F_{ry} \quad (5.17)$$

By assume that relationship between tire slip angle and tire lateral force are linear equation, the F_{fy} and F_{ry} can evaluate from equation 5.18 and 5.19.

$$F_{fy} = \alpha_f \cdot K_f \quad (5.18)$$

$$F_{ry} = \alpha_r \cdot K_r \quad (5.19)$$

From equation 5.3, 5.5, 5.7, 5.8, and 5.9, the α_f and α_r can be evaluated. Since the calculation done on assumption that steering angle and vehicle side-slip angle are small, the evaluation for α_f and α_r can be simplified. Then substitute the result into equation 5.18 and 5.19 to get equation 5.20 and 5.21.

$$F_{fy} = K_f\left(\delta - \beta - \frac{r \cdot WB_f}{V}\right) \quad (5.20)$$

$$F_{ry} = K_r\left(-\beta + \frac{r \cdot WB_r}{V}\right) \quad (5.21)$$

Substitute equation 5.20 and 5.21 into equation 5.16 and 5.17. Then rearrange them into 2 linear equation form as equation 5.22.

$$\begin{Bmatrix}\dot{\beta}\\ \dot{r}\end{Bmatrix} = [A]\begin{Bmatrix}\beta\\ r\end{Bmatrix} + [B]\{\delta\} \quad (5.22)$$

Because the calculation done on assumption of steady-state cornering, therefore the vehicle side-slip angle and yaw rate are constant. Then equation 5.22 will be equal to 0. Solve equation 5.22 for β and r by using equation 5.23.

$$\begin{Bmatrix}\beta\\ r\end{Bmatrix} = -[A]^{-1}[B]\{\delta\} \quad (5.23)$$

Therefore the Stability Factor, vehicle side-slip angle gain, and vehicle yaw-rate gain can be calculated from equation 5.24 to 5.26.

$$SF = \frac{m}{2(WB)^2}\left(\frac{WB_r}{K_f} - \frac{WB_f}{K_r}\right) \quad (5.24)$$

$$\frac{\beta}{\delta} = \frac{WB_r}{WB\left(1 + SF \cdot V^2\right)}\left(1 - \frac{WB_f \cdot m \cdot V^2}{2 \cdot WB \cdot WB_r K_r}\right) \quad (5.25)$$

$$\frac{r}{\delta} = \frac{V}{WB\left(1 + SF \cdot V^2\right)} \quad (5.26)$$

The calculation for truck trailer will use the same vehicle configuration; therefore the WB, WB_f, WB_r, and m are all the same. Cornering stiffness of front and

rear tire (K_f ,K_r) are evaluate from calculation result in figure 5.13. The K_f will be refer to 2 of normal tire. For the rear tire of normal dual tires will be 8 times more than normal single tire. For WBS rear tire, it will be 4 times more than single WBS tire.

K_f	K_r dual	K_r WBS
5,500	22,000	18,000

Table 5.5 Cornering stiffness that use in bicycle model calculation.

To see the effect of different vehicle configuration, the calculation will be done with various different CG position. But in every calculation will maintain total mass of truck and tires properties. The calculation results show in figure 5.18 to 5.23.

Total mass (kg.)	Weight distribution ratio (front : rear)
25,000	23 : 77
25,000	20 : 80
25,000	17 : 83

Table 5.6 Parameters for calculate vehicle dynamics.

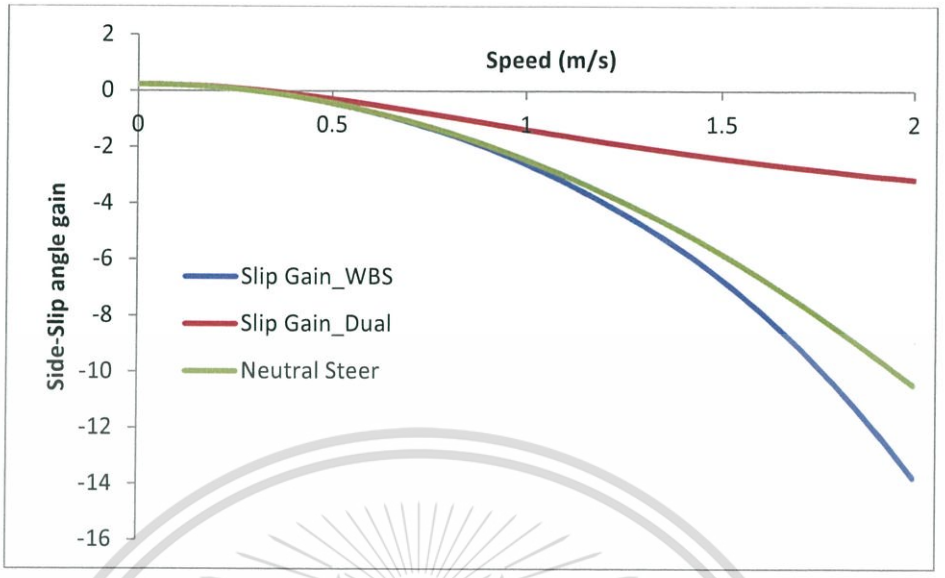

Figure 5.18 Vehicle side-slip angle gain for 23:77

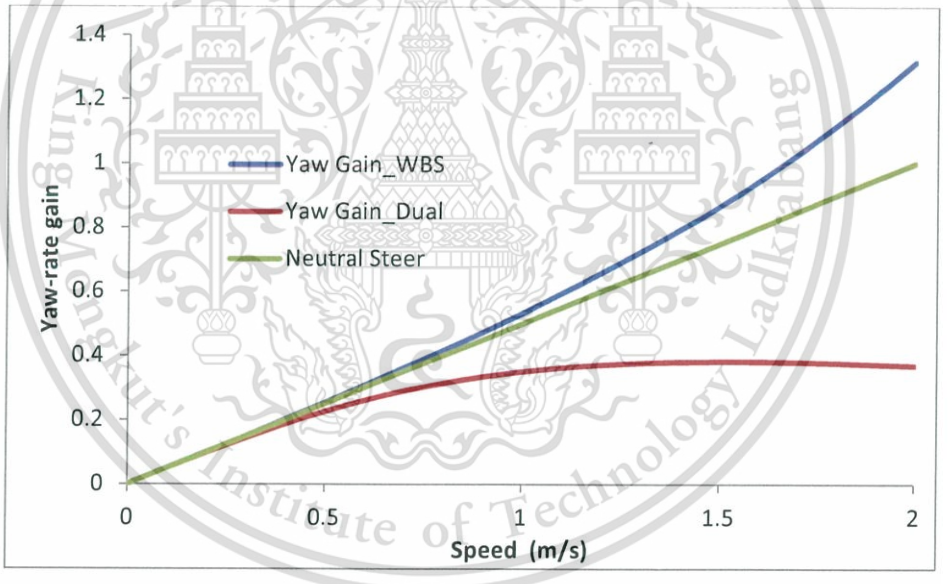

Figure 5.19 Yaw-rate gain for 23:77

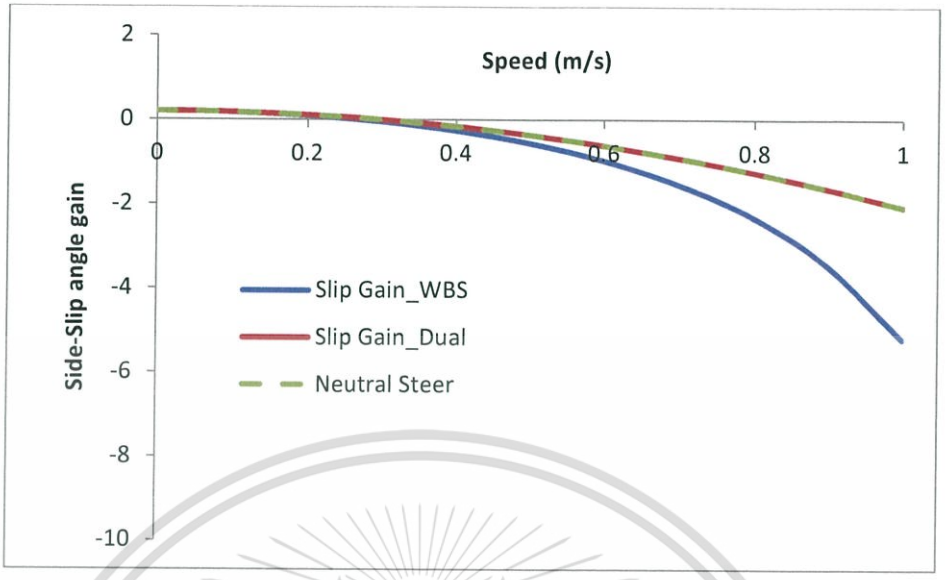

Figure 5.20 Vehicle side-slip angle gain for 20:80

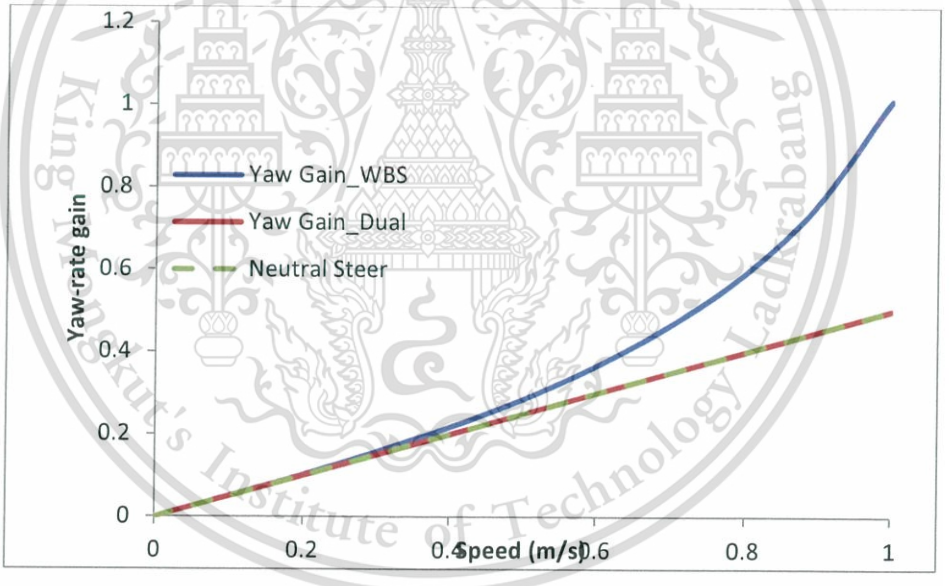

Figure 5.21 Yaw-rate gain for 20:80

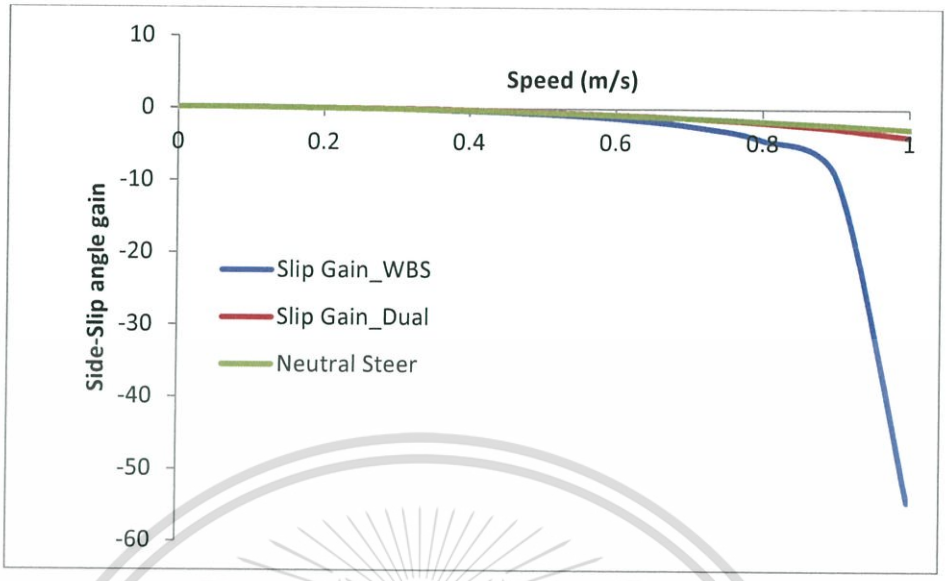

Figure 5.22 Vehicle side-slip angle gain for 17:83

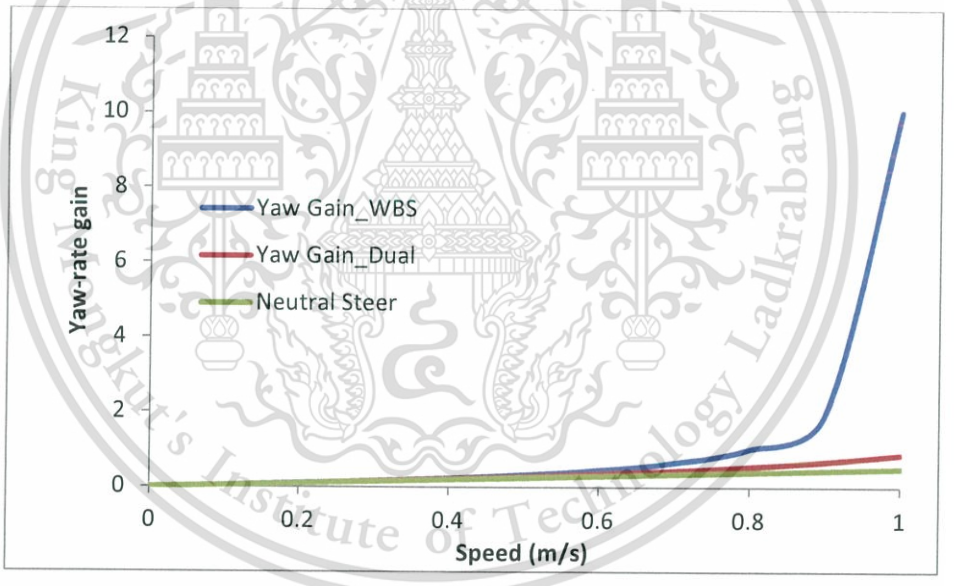

Figure 5.23 Yaw-rate gain for 17:83

From table 5.5, the cornering stiffness of WBS tire less than Dual tires, when substitute into equation (5.24) the Stability Factor (SF) of WBS tire will be less than Dual tires. This means when compare to Dual tires, WBS tire tend to have Over-Steer. In figure 5.18 to 5.23, Side-Slip Angle gain and Yaw-Rate gain of WBS tire and Dual tires are comparing with Neutral Steering. In figure 5.20 and 5.21 show that at 20:80

weight distribution, the Dual tires can give similar to Neutral Steering. This means the Dual tires give better vehicle control when compare with WBS tire. In figure 5.18 and 5.19 show that if weight distribution of vehicle is 23:77, the WBS tire can approach to Neutral Steering better than Dual tires. This means the WBS tire can gives better control at this weight distribution.

5.5 Result Discussion

Refer to testing result in lecture document, the calculation result of Proposed Model could predict the lateral force accurately. The prediction of cornering stiffness is accurate. But for self-aligning torque prediction still not accurate.

According to Yang's research, the calculation result at 500 N and 750 N is very accurate at low slip angle. At slip angle before fully slip is inaccurate, the error is 6.23% compare with testing result. At full slip, the calculation gives slightly error at 0.6%. The overall calculation accuracy is better than the simulation result that done by using constant friction.

But at 1000 N the result at low slip is not accurate, even worse than FEA. Refer to footprint testing result in [2], at low to mid vertical load, footprint area will increase in size but maintain its aspect ratio and pressure distribution in parabola form. But at higher vertical load, the footprint shape will not maintain its aspect ratio and pressure distribution is not in parabola form anymore. This may causes the calculation that based on parabola shape of pressure distribution gives not accurate result.

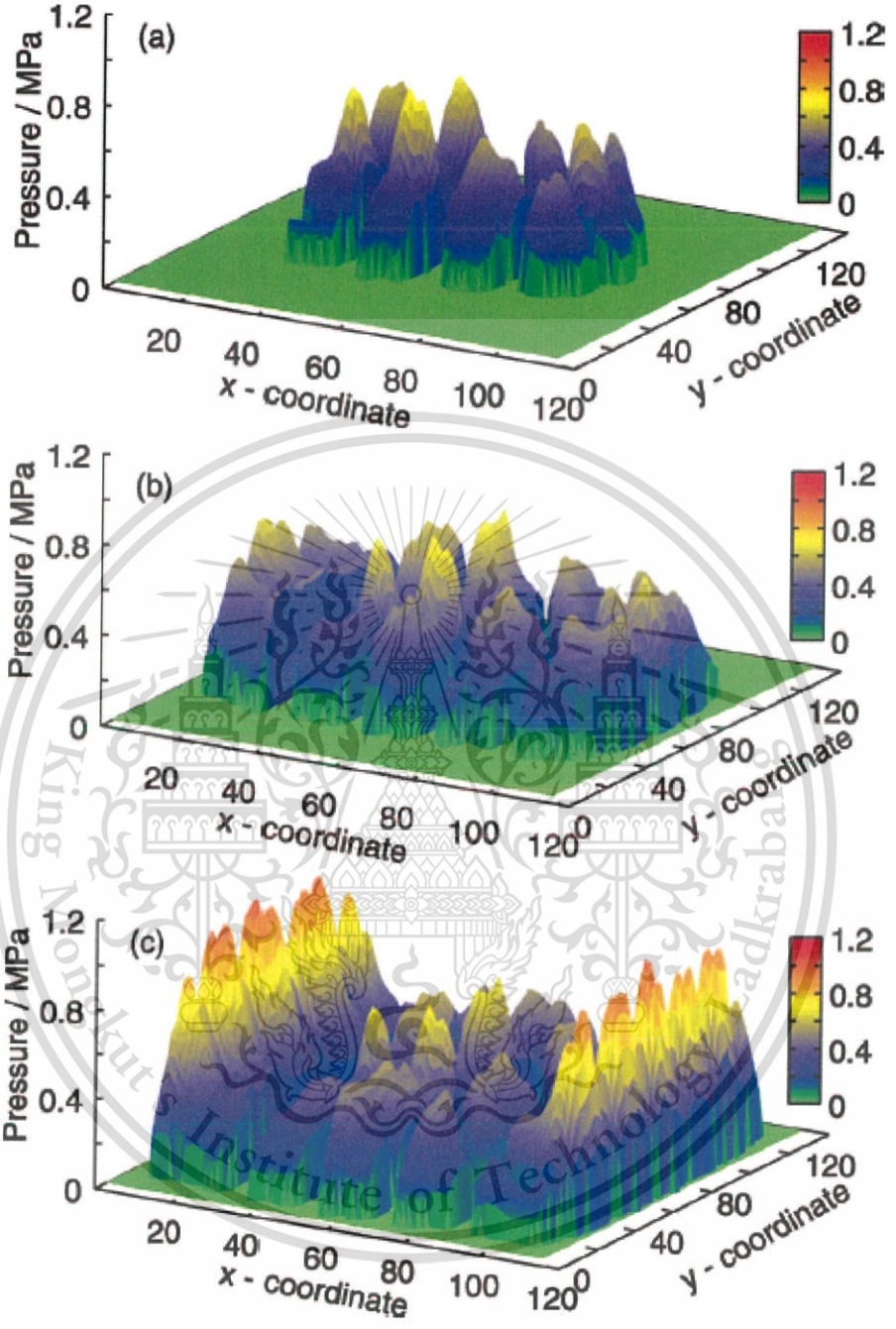

Figure 5.24 Footprint testing result at different vertical load **[19]**

Since the pressure distribution in footprint can analyze by FEA with low calculation time, the further improvement that author suggest is to analyze footprint and

pressure distribution by FEA first, then transfer the result into Proposed Model. The working procedure should looks like figure 4.11.

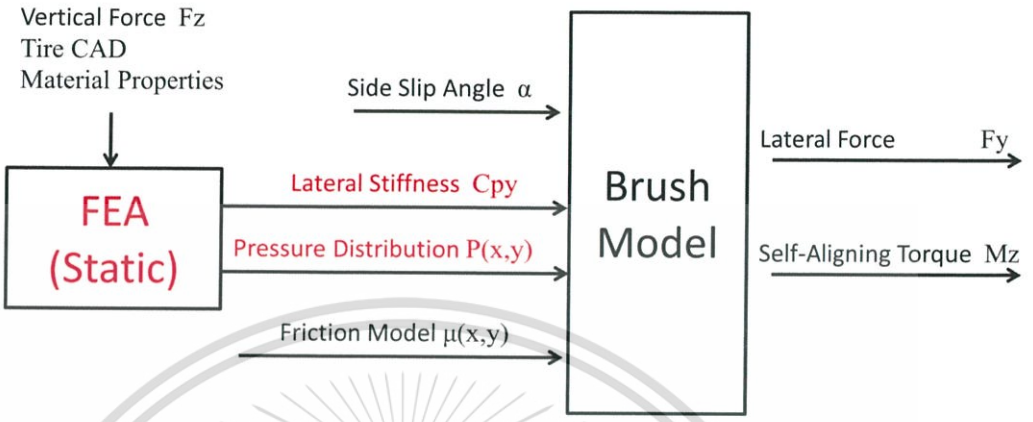

Figure 5.25 Proposed Tire Modeling diagram, working with FEA

The calculation result of Wide-Based-Single tire show that it gives higher maximum lateral force than Normal Dual tires. But the cornering stiffness of WBS tire is less than Normal Dual tires. For self-aligning torque, WBS tire generates less torque than Normal Dual tires. The self-aligning torque calculation still questionable, but both WBS tire and Normal Dual tires are use for rear wheel. This means the self-aligning torque is not gives effect to the usage of those tire.

The calculation for vehicle dynamics show that WBS tire tend to make vehicle over-steer when compare to normal dual tires. This effect occurred because WBS tire has less cornering stiffness when compare to normal dual tire. This may cause by the contact area of WBS is less than normal dual tire. But this problem can solve by changing the configuration of "Fifth Wheel Coupling" to change weight distribution of the truck.

CHAPTER 6

CONCLUSION AND RECOMMENDATION

6.1 Result Conclusion

The testing results of the tires that have different width prove that the friction coefficient doesn't constant, and can be affected by tire geometry. The calculation results also prove that calculations that made out with constant friction coefficient are unacceptable. The calculation results show the including of "Cold-Hot Friction Law" in brush model can maintain accuracy prediction at low slip angle. Also reduce the error at high slip angle in both before and after full slip. The error reduces from 11% (simulation result) to 6.23% at 4 degree of slip angle, and reduces from 8% to 0.6% at full slip, refer to testing result. The improvement also represents the friction loss phenomenon in tire and gives different maximum lateral force for different tire width which classical model has never been able to archive. But the "Cold-Hot Friction Law" needs additional testing for the friction in both "cold" and "hot" condition at different velocity and ambient temperature. The testing procedure and data analysis are complicate. Please see [18] for testing and analysis procedure details.

The comparison between WBS tire and normal dual tires show that WBS tire gives 18% less cornering stiffness due to less contact area. This may result that truck tend to over-steering when evaluate with linear tire model and bicycle model. The problem can be resolve by adjusting the "Fifth Wheel Coupling" to move CG of vehicle for around 3% to frontal.

6.2 Recommendation

From the research, the pneumatic tire contact mechanism is consists of many complicate modeling. The pneumatic tires are normally constructed from either rubber-steel or rubber-fabric composite material. The rubber also nonlinear elastic material, it actually consists of Hyperelastic and Viscoelastic properties. But for Brush Model, the nonlinear model of material properties does not give high effect to lateral stiffness. But

Viscoelastic material has strongly affected by temperature and will gives effect to friction model. Nonlinear model of lateral stiffness also not receive any affect neither from contact area shape nor size.

In the term of friction model, the Coulomb's friction model is not enough to explain rubber friction. The contact mechanic of Viscoelasticity in rubber have greatly affected by temperature. During the tire usage, the hysteresis in thread will generate heating energy and result in temperature increase in thread. After done this research, author strongly recommends including "Cold-Hot Friction Law" into friction modeling. Since the calculation result can gives both effect of contact shape and reduction of lateral force at full-slip. Those effects are occurred only when changed the constant friction coefficient into function of friction model. Many commercial FEA programs also support the User-Defined Function, so the friction model can be able to include in to FEA programs.

As the result shows that at 1000 N. of vertical load, the calculation result gives error at low slip angle. The cornering stiffness is too high when compare with FEA and testing results. But at full-slip the result is quite accurate. This means the contact model may correct but the pressure distribution in foot print shape is not correct. As show in figure 5.10, at low vertical load the pressure distribution shape is near with the elliptical parabola. But at higher vertical load the pressure distribution will not in the shape of elliptic parabola. The pressure is mainly distributed to the side wall zone of the tire. This occurred because the roundness of tire cross-section makes the mid-zone of the tire contact the pavement first. But at the higher load, the side-zone will finally contact with the pavement and they have higher stiffness. This will result in pressure distribution at low load will majorly high at mid-zone but at high load it will high at size-zone.

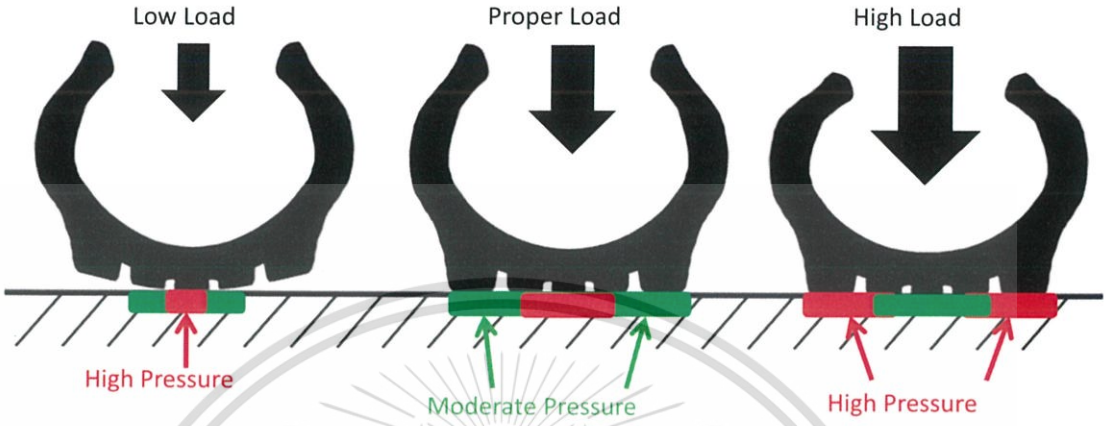

Figure 6.1 Comparison of tire section at different vertical load

The footprint and pressure distribution that used throughout this research is artificial generated from simple mathematical equation. In real life, foot print and pressure distribution are comes in complex shape and sensitive with many parameters, such as thread shape, inflation pressure, tire structure, etc. In commercial FEA programs are capable with this calculation, the calculation also only nonlinear static, this means the calculation time in not high (~15 min). Author suggests that in designing process, the FEA is an option to take place in this calculation.

The footprint and pressure distribution is strongly effect to cornering stiffness, maximum lateral force, slip distance, and lateral force at full-slip. Therefore if footprint shape, size, or pressure is wrong, the result also gives high error. The smaller contact area will gives higher pressure but will result in lower cornering stiffness because of the lower deformation of thread at same slip angle. At same size but wider contact area, the thread deformation that affected by slip angle also lowers than narrow tire. This will result in lower slip distance, and gives result that wider tire can generate higher lateral force because of less Flash Temperature and slip distance.

The truck trailer may tend to over-steer if use WBS tire. This problem can be solved by changing the configuration at "Fifth-Wheel Coupling" to move the CG of

overall load a little frontal. Therefore the actual usage of WBS in truck trailer may not have any effect with cornering performance if have a proper adjustment.

For better vehicle dynamics evaluation, the calculation model should be nonlinear refer to nonlinear tire model. In this article gives only rough prediction in vehicle dynamics evaluation. The effect of maximum lateral force and traction loss of the tire are not included in the calculation. If the nonlinear vehicle modeling has used instead, the result may differ.

REFERENCE

[1] Transport Statistic Sub-Division. [Online] Department of Land Transport, 2016. [Cited: 06 16, 2017.] http://apps.dlt.go.th/statistics_web/vehicle.html.

[2] Rubber friction and tire dynamics. Persson, B.N.J. 1, Julich : Journal of Physics: Condensed Matter, 2010, Vol. 23.

[3] Experimental Validation of Terrain-Aware Rollover. Sittikorn Lapapong, Alexander A. Brown, and Sean N. Brennan. Pennsylvania : 10th International Symposium on Advanced Vehicle Control, 2010.

[4] Schmid, Markus. Tire Modeling for Multibody Dynamics Applications. s.l. : University of Wisconsin-Madison, 2011.

[5] Effect of Single Wide Tires and Trailer Aerodynamics on Fuel Economy and NOx Emissions of Class 8 Line-Haul Tractor-Trailers. L. Joseph Bachman, Anthony Erb, and Cheryl L. Bynum. s.l. : Society of Automotive Engineering (SAE) International, 2005. Paper Number 05CV-45.

[6] Factors AffectingTruck Fuel Economy. s.l. : Goodyear Commercial Tire Systems, 2008.

[7] Michelin Viewpoint on Wide Base Singles and Other Future Truck Tyre Types. Penant, C. Delft : 7th International Symposium on Heavy Vehicle Weights & Dimensions, 2002.

[8] Department, Engineerin. New Generation Wide Base Single Tires. Virginia : American Trucking Associations.

[9] Yang, Xiaoguang. Finite Element Analysis and Experimental Investigation of Tyre Characteristic for Developing Strain - Based Intelligent Tyre System. Burmingham : The University of Burmingham, 2011.

[10] Pacejka, Hans B. Tire and Vehicle Dynamics. s.l. : Elsevier Ltd., 2002. ISBN 0-7506-5141-5.

[11] William F. Milliken and Douglas L. Milliken. Race Car Vehicle Dynamics. Pennsylvania : Society of Automotive Engineering, Inc., 1995. ISBN 1-56091-526-9.

[12] A.J.C. Schmeitz, I.J.M. Besselink, J. de Hoogh, H. Nijmeijer. Extending the Magic Formula and SWIFT tyre models for inflation pressure changes. Eindhoven : Eindhoven University of Technology, 2005.

[13] Chikamori, Sunao. Vehicle Handling Dynamics. Basic/Advanced Engineering for Automotive Course. Tokyo : Society of Automotive Engineers of Japan, 2015.

[14] Prediction of Automobile Tire Cormering Force Characteristics by Finite Element Modeling and Analysis. Ergin Tonuk, Y. Samim Unlusoy. 79, Ankara : Elseviel, 2001.

[15] Rubber friction for tire tread compund on road surfaces. B Lorenz, B N J Persson, G Fortunato, M Giustiniano and F Baldoni. 095007, Julich : Journal of Physics: Condensed Matter, 2013, Vol. 25.

[16] Rubber Friction and Tire Dynamics: A Comparison of Theory with Experimental Data. Michael Selig, Boris Lorenz, Dirk Henrichmoller, Karsten Schmidt, Andrew Ball, B.N.J. Persson. 4, pp. 216-262, s.l. : Tire Science and Technology, TSTCA, 2014, Vol. 42.

[17] Steen, R.van der. Tire/road friction modeling. s.l. : Eindhoven University of Technology, 2007.

[18] Rubber friction: role of the flash temperature. Persson, B.N.J. 32, Julich : Journal of Physics: Condensed Matter, 2006, Vol. 18.

[19] On the Theory of Rubber Friction. Persson, B.N.J. 445-454, Julich : Surface Science, 1997, Vol. 401.

[20] W. Edward Gettys, Frederick J. Keller, Malcolm J. Skove. Physics: Classical and Modern. s.l. : McGraw-Hill, Inc., 1989. ISBN 0-07-033523.

[21] Peterson, Eric Wade. Tire-Road Friction Coefficient Estimation Using a Multi-scale, Physic-based Model. Virginia : Virginia Polytechnic Institute and State University, 2014.

[22] Rubber friction, thread deformation and tire traction. Gert Heinrich, Manfred Kluppel. 7-8, Dresden : Elsevier, 2008, Vol. 265. ISSN 0043-1646.

[23] Tire Cornering Simulation using Explicit Finite Element Analysis Code. Koishi, M., K. Kabe, and M. Shiratori. 2, s.l. : Tire Science and Technology, 1998, Vol. 26. ISSN 0090-8657.

[24] Wong, J.Y. Theory of Ground Vahicles 4th ed. s.l. : John Wiley & Sons, Inc., 2008. ISBN 0-470-17038-7.

[25] D.Bastow, G. Howard, J. P. Whitehead. Car Suspension and Handling. s.l. : SAE, 2004. ISBN 0-7680-0872-7.

APPENDIX A

QUESTION AND ANSWER FROM THESIS DEFENSE EXAMINATION

1. You used an oval contact area assumption in the tire model. I'd like to ask the reason why the oval contact area assumption induces better estimation than the rectangle contact area assumption. Please explain the reason, in your opinion.
   Did you try to use bi-parabola pressure model for the rectangle contact area assumption to express pressure distribution in lateral direction?

$$P(x,y) = 8P_{\max}\left(\frac{x}{l}\right)\left(1-\frac{x}{l}\right)\left(\frac{y}{b}\right)\left(1-\frac{y}{b}\right)$$

   Answer: The calculation results are improved by oval contact area assumption because the pressure distribution assumption in Classical Brush Model is distribute only in x-direction. But the testing result shows that pressure also distribute in y-direction as well.

   I have not tried the bi-parabola pressure model for the rectangle contact area yet. But it may give similar result since the difference with oval contact area shape is that it has edges. At the edges of contact area have very low pressure act on them. Therefore the calculation result may similar with oval contact area shape.

2. In your vehicle dynamics analysis, WBS tire induces over-steer characteristics; heading to the inside of the corner. But as you know, usually, front wheel drive vehicle shows under-steer characteristics; heading to the outside of the corner. Specially, low front weight ratio tends to under-steer characteristics. Could you please explain the reason why low-lateral stiffness of rear tire results in the over-steer characteristics?
   Usual track is "front wheel drive" and bicycle is "rear wheel drive". Is your bicycle model "rear wheel drive" or "front wheel drive"?

Answer: In the case of WBS tire, rear wheel of the bicycle model consist of 4 tires inside. After some calculations, it will show that each tire will subjected to load at double of front tire. And if we calculate for Dual Tires, each tire will be subjected to same load as front tire. This means at 20:80 weight ratio, 2:8 tires can generate appropriate force for Neutral Steer. From Figure 5.13, when compare WBS with Dual Tire, we can see clearly that at low Slip Angle WBS generate less Lateral Force when compare with Dual Tires. That means for WBS tires, rear tires are generate less force and will tend to loss their traction.

In my calculation, the force in Longitudinal Axis assumed to be 0. Therefore the calculation is not considering about the driving or braking force. As shown in Figure 5.16 - 5.17 and Equation 5.15. In conclusion, my calculation does not concern that the vehicle is Front or Rear Wheel Drive.

3. The lateral stiffness of WBS tire changes with dimensions and structure of tire and air pressure. Did you use data with one of commercial product?
   Do you have any suggestions to improve lateral stiffness of WBS tire?

   Answer: The data that included for calculation in this research is the contact length and contact width of the footprint that provided from company. The contact shape may differ if the tire dimension, tire structure, and inflation pressure are changed. Since the testing result as the footprint shape is the output of those parameter, therefore the effect of those parameter will represent in different contact shape. But the Lateral Stiffness calculation in this research is concern only properties of thread element, that different from the testing at very high Slip Angle. If tire deform more at higher Slip Angle, the dimension and structure of the tire are also involve with Lateral Stiffness, as well as the inflation pressure.

   The Lateral Stiffness is the parameter that majorly affected by tire structure and material properties. If the structure of the tire has more reinforcement (steel wire, etc.) the structure of the tire will be stiffer. As well as the higher inflation pressure

also gives higher Lateral Stiffness. But the stiffer tire also gives lower contact area. In result the Lateral Stiffness if the tire may increase, but the Cornering Stiffness may reduce due to smaller contact area.

To compromise these parameters, in designing process needs to acquire the highest stiffness that also gives high contact area at designing vertical load.

4. How can you derive the μ_{hot} when your references are not provided this data?

   Answer: Since those researches are provided the testing results of pure Slip-Force on testing machine. The evaluation for μ_{hot} can be done refer to Figure 4.12. At higher Slip Angle, the slip distance also increases. The higher slip distance will makes the μ_{eff} converge to μ_{hot}. Therefore the calculation for μ_{hot} can be done by use the Lateral Force at Full-Slip divided by vertical load.

5. For the further usage of this research, how can we apply the Proposed Model with nonlinear vehicle dynamics analysis?

   Answer: The relationship between Slip Angle – Lateral Force and be use instead of testing result. That means we can use this calculation result with "Magic Formula" to get the constants to use with "MF-Tire Model" and applied these constant as Tire Properties for commercial code, i.e. "ADAMS/Cars", "Car Sim", etc. The simulation code can use these parameters for calculate with fully-dynamics model and nonlinear tire modeling. This methodology can save cost for testing and reduce calculation time for FEA. Overall procedure also not requires the prototype.

APPENDIX B

MATLAB CODE FOR "CLASSIC BRUSH MODEL"

```
close all
clear all
clc

%================  Tire Parameters ======================

l=0.067;              %Contact Length (m)
b=0.134;              %Contact Width (m)
Fz=750;               %Normal Load (N)
ky=38.857e6;          %Lateral Stiffness (N/m)
mu=1;                 %Froction Coeff.
a=b*l;                %Reference Area (m^2)

%=========================================================

l=a/(b);
pm=3*Fz/2/l/(b);      %Maximum pressure

%================  Variations ============================

F=[];                                 %Metrix of total force
x=0:0.001:l;                          %Create metrix of x-axis position
p=4*pm*(x/l).*(1-(x/l));              %Pressure Deistribute calculation
Ff=p*b*mu;                            %Friction force
alphad=0:0.1:50;                      %Create alpha
alpha=alphad.*pi()/180;               %Convert to rad.
for n=1:size(alpha,2)
    Ft=b*ky*(x)*tan(alpha(n));        %Restoring Force
    intFt=Ft;
    for m=1:size(intFt,2)
        if Ft(m)>Ff(m)
            intFt(m)=Ff(m);
```

```
        end
    end
    F=[F,(sum(intFt))*0.001];

    %============= Pressure Distb. Plot ======%
    if(alphad(n)==3)
        figure(1);
        L1=plot(x,Ff,'-.');
        hold on;
        L2=plot(x,Ft);
        set(gca,'XDir','reverse')
        title('X-Position and Force')
        xlabel('Distance from leading edge (m)')
        ylabel('Force (N)')
        grid on;
        hold off;
        legend([L1,L2],'Friction Force','Restoring Force')
    end
end

figure(2);
L=[plot(alphad(1:100),F(1:100),'r')];
hold on;
title('Slip angle and Force')
xlabel('Slip angle (deg)')
ylabel('Force (N)')
grid on

test1=[0    1   2   3   4   5   6   7   8];
test2=[0    320 500 585 630 660 670 685 690];
L=[L;plot(test1,test2)];
legend(L,'Classic BrushModel','Testing Result')
```

APPENDIX C

MATLAB CODE USED IN VALIDATION WITH YANG'S RESEARCH

```
clear all
close all
clc

%================  Tire Parameters ======================
l=0.0754;        %Contact Length (m)
b=0.1514;        %Contact Width (m)
Fz=750;          %Normal Load (N)
ky=63.69e6;      %Lateral Stiffness (N/m)
r0=0.01;         %0.2D (m) Average contact area diameter in micro-scale
%=========================================================

res=0.001;
bFactor=[0.9:0.1:1.1];      %Factor to change contact width for compare
alphad=0:0.1:50;             %Create alpha
alpha=alphad.*pi()/180;      %Convert to rad.
x=0:res:l;                   %Create metrix of x-axis position
Fprog=[];
Wprog=[];
Gcol=['b','r','k'];          %Create Graph Colour
mu12=[0.85 1];               %Hot and Cold Mu
mu=mu12(2);                  %Cold Froction Coeff.
L=[];
LM=[];

for o=1:size(bFactor,2)

%================= Parameters calculations ===============
y=(-1)*b*bFactor(o)/2:res:b*bFactor(o)/2;    %Create metrix of y-axis
position
pm=8*Fz/pi/l/(b*bFactor(o));                 %Maximum pressure
%=========================================================
```

```
%================ Variations ============================
F=[];                                          %Metrix of total force
M=[];                                          %Metrix of total moment
p=zeros(size(x,2),size(y,2));
for n=1:size(y,2)
    for m=1:size(x,2)
        p(m,n)=pm-(pm*((((x(m)-
(l/2))/(l/2))^2)+(((y(n))/(b*bFactor(o)/2))^2)));          %Pressure
Distribution
        if p(m,n)<0
            p(m,n)=0;
        end
    end
end
Ff=p*mu;                                       %Friction force
for n=1:size(alpha,2)
    Ft=ky*(x)*tan(alpha(n));                   %Adhesive Zone Force
    intFt=zeros(size(x,2),size(y,2));
    sumx=[];
    sumM=[];
    for s=1:size(y,2)
        intersect=0;
        for r=1:size(x,2)
            if Ft(r)>Ff(r,s)
                if intersect==0
                    r_ref=x(r)*tan(alpha(n));          % Detect the
initial slip
                    intersect=x(r);
                    intFt(r,s)=Ff(r,s);
                else
                    Ffdis=Ff(r,s)/ky/b/bFactor(o);     %Displacement
calculation
                    dr=abs(r_ref-Ffdis);           %Slip Distant
%==============Cold-Hot Friction Law==================
                    mueff=(mu12(2)*exp(-dr/r0))+(mu12(1)*(1-exp((-
dr/r0))));
                    intFt(r,s)=Ff(r,s)*mueff/mu12(2);
```

```
                end
            else
                intFt(r,s)=Ft(r);
            end
        end
        sumx=[sumx,sum(intFt(:,s))];
        sumM=[sumM,sum(intFt(:,s).*(x(:)-(l/2)))];
    end

    F=[F,sum(sumx)*res*res];
    M=[M,sum(sumM)*res*res];
    %============= Pressure Distb. Plot ======%
    if(alphad(n)==3)
        figure(1);
        subplot(2,1,1);
        L1=plot(x,Ff(:,ceil(size(y,2)/2)),'-.');
        hold on;
        L2=plot(x,Ft);
        set(gca,'XDir','reverse')
        title('X-Position and Force')
        xlabel('Distance from leading edge (m)')
        ylabel('Force (N)')
        grid on;
        legend([L1,L2],'Maximum Friction Force','Lateral Slip Force')
        figure(3);
    end
    if(alphad(n)==3)
        figure(o+4);
        surf(intFt);
    end
end
%================= Plot Force Graph ================%
figure(1);
subplot(2,1,2)
plot(x,p(:,ceil(size(y,2)/2)));
hold on;
set(gca,'XDir','reverse')
```

```
title('X-Position and Pressure')
xlabel('Distance from leading edge (m)')
ylabel('Pressure (Pa)')
grid on;
figure(2)
L=[L;plot(alphad(1:100),F(1:100),Gcol(o))];
hold on;
title('Slip angle and Lateral Force')
xlabel('Slip angle (deg)')
ylabel('Force (N)')
grid on
figure(4)
LM=[LM;plot(alphad(1:100),M(1:100),Gcol(o))];
hold on;
title('Slip angle and Self Aligning Torque')
xlabel('Slip angle (deg)')
ylabel('Torque (N-m)')
grid on
Fprog=[Fprog max(F)];
Wprog=[Wprog b*bFactor(o)];
fprintf('Width=%d mm,MaxForce=%d kN\n',1000*b*bFactor(o),max(F)/1000);
end
figure(2)
legend(L,'90% width','100% width','110% width')
figure(4)
legend(LM,'90% width','100% width','110% width')
figure(3)
plot(Wprog,Fprog)
title('Footprint Width and Maximum Lateral Force')
xlabel('Footprint Width (m)')
ylabel('Force (N)')
```

AUTHOR BIOGRAPHY

Author:	Mr.Jittrin Nimitpermpoon
Degree:	Master of Engineering
Date of Graduation:	27th July 2017
Date of Birth:	26th December 1989
Place of Birth:	Bangkok,Thailand

Undergraduate and Graduate Education:

Master of Engineering in Automotive Engineering, International College

King Mongkut's Institute of Technology Ladkrabang, Bangkok, 2016

Bachelor degree in Mechanical Engineering, Faculty of Engineering

King Mongkut's Institute of Technology Ladkrabang, Bangkok, 2011

Major: Automotive Engineering

Presentations and Publications:

[1] J. Nimitpermpoon, K. Tongdee, K. Kowaranon, C. Charoenphonphanich, P. Karin, "Carbon Fiber Wheel for Future Vehicle", International Conference of Automotive Technology for Young Engineers (ICATYE) 2012-2013, 8 March 2013, Japan

[2] J. Nimitpermpoon, M. Pimsarn, H. Yamaura, S. Lapapong, "Nonlinear Tire Dynamics Based on the Cold-Hot Friction Law", Technical Paper, 2017 JSAE Annual Spring Congress, 24-26 May 2017, Yokohama, Japan.